nature medicine

LETTERS

https://doi.org/10.1038/s41591-019-0650-9

# Simultaneous detection of genotype and phenotype enables rapid and accurate antibiotic susceptibility determination

Roby P. Bhattacharyya[1,2,10], Nirmalya Bandyopadhyay[1], Peijun Ma[1], Sophie S. Son[1], Jamin Liu[1], Lorrie L. He[1], Lidan Wu[3], Rustem Khafizov[3], Rich Boykin[3], Gustavo C. Cerqueira[1,4], Alejandro Pironti[1], Robert F. Rudy[1], Milesh M. Patel[1], Rui Yang[1], Jennifer Skerry[5], Elizabeth Nazarian[6], Kimberly A. Musser[6], Jill Taylor[6], Virginia M. Pierce[5], Ashlee M. Earl[1], Lisa A. Cosimi[7], Noam Shoresh[1], Joseph Beechem[3], Jonathan Livny[1,10] and Deborah T. Hung[1,8,9,10]*

**Multidrug resistant organisms are a serious threat to human health[1,2]. Fast, accurate antibiotic susceptibility testing (AST) is a critical need in addressing escalating antibiotic resistance, since delays in identifying multidrug resistant organisms increase mortality[3,4] and use of broad-spectrum antibiotics, further selecting for resistant organisms. Yet current growth-based AST assays, such as broth microdilution[5], require several days before informing key clinical decisions. Rapid AST would transform the care of patients with infection while ensuring that our antibiotic arsenal is deployed as efficiently as possible. Growth-based assays are fundamentally constrained in speed by doubling time of the pathogen, and genotypic assays are limited by the ever-growing diversity and complexity of bacterial antibiotic resistance mechanisms. Here we describe a rapid assay for combined genotypic and phenotypic AST through RNA detection, GoPhAST-R, that classifies strains with 94–99% accuracy by coupling machine learning analysis of early antibiotic-induced transcriptional changes with simultaneous detection of key genetic resistance determinants to increase accuracy of resistance detection, facilitate molecular epidemiology and enable early detection of emerging resistance mechanisms. This two-pronged approach provides phenotypic AST 24–36 h faster than standard workflows, with <4 h assay time on a pilot instrument for hybridization-based multiplexed RNA detection implemented directly from positive blood cultures.**

Current gold-standard AST assays that measure growth in the presence of an antibiotic, while slow, directly answer the key question of whether the antibiotic inhibits pathogen growth. By contrast, newer genotypic approaches[6] fall short of universal AST because of our incomplete knowledge of the innumerable resistance-causing genes and mutations across all pathogens and antibiotics, and the interactions of these genetic factors with diverse genomic backgrounds within any given bacterial species[7–9]. While the genomics revolution has undeniably transformed our understanding of antibiotic resistance[10–12], as a clinical diagnostic, whole-genome sequencing (WGS) remains technically demanding, costly and slow; and the complexity, variability and continuing evolution of bacterial genomes under ongoing antibiotic exposure pose serious challenges to predicting susceptibility accurately enough to direct patient care[9,13,14]. These shortcomings have motivated several new approaches that focus on faster phenotypic AST, including rapid automated microscopy[15], ultrafine mass measurements[16] and others[17–19].

Among current multidrug resistant organisms (MDROs), carbapenem-resistant organisms are the most alarming, as their resistance to this broad-spectrum antibiotic class often leaves few to no treatment options[20]. Yet phenotypic carbapenem resistance detection can be challenging, as some carbapenemase-producing strains may be mistakenly identified as susceptible by current phenotypic assays[21] while failing clinical carbapenem therapy[22]. Newer multiplexed PCR assays can detect several common carbapenemases in carbapenem-resistant *Enterobactericeae* (CRE)[6], yet these genotypic approaches miss a substantial fraction of CRE isolates (13–68%) with unknown or noncarbapenemase resistance mechanisms[8,23]. For non-*Enterobacteriaceae*, these alternative genetic resistance mechanisms account for the vast majority of resistance; just 1.9% of over 1,000 carbapenem-resistant *Pseudomonas* surveyed in 2017 by the US Centers for Disease Control harbored known carbapenemases[23]. These challenges have left clinical microbiology laboratories still seeking consensus on how to best apply the multiple possible workflows for detecting carbapenem resistance[24,25], including phenotypic[26], genetic[24] and biochemical[25] assays.

GoPhAST-R (combined genotypic and phenotypic AST through RNA detection) is a diagnostic approach that can detect both genotype and phenotype in a single rapid assay, allowing integration of all information and simultaneously informing both resistance prediction and molecular epidemiology. GoPhAST-R detects specific messenger RNA expression signatures in bacteria after brief

[1]Infectious Disease and Microbiome Program, Broad Institute of Harvard and MIT, Cambridge, MA, USA. [2]Infectious Diseases Division, Department of Medicine, Massachusetts General Hospital, Boston, MA, USA. [3]NanoString Technologies, Inc., Seattle, WA, USA. [4]Present address: Personal Genome Diagnostics, Ellicott City, MD, USA. [5]Microbiology Laboratory, Department of Pathology, Massachusetts General Hospital, Boston, MA, USA. [6]Wadsworth Center, New York State Department of Health, Albany, NY, USA. [7]Infectious Diseases Division, Department of Medicine, Brigham and Women's Hospital, Boston, MA, USA. [8]Department of Genetics, Harvard Medical School, Boston, MA, USA. [9]Department of Molecular Biology and Center for Computational and Integrative Biology, Massachusetts General Hospital, Boston, MA, USA. [10]These authors jointly supervised this work: Roby P. Bhattacharyya, Jonathan Livny, Deborah T. Hung. *e-mail: hung@molbio.mgh.harvard.edu

antibiotic exposure; susceptible cells that are stressed on antibiotic exposure are transcriptionally distinct from resistant cells that are not, agnostic to resistance mechanism[17]. mRNA is uniquely informative in this regard, as it encodes genotypic information in its sequence and phenotypic information in its abundance. Here we show that multiplexed hybridization-based quantification of transcriptional responses within minutes of antibiotic exposure can distinguish susceptible from resistant organisms. We demonstrate this approach for three major antibiotic classes in common clinical use—fluoroquinolones, aminoglycosides and carbapenems—in five pathogens with a propensity for multidrug resistance through diverse mechanisms. We describe a generalizable process to extend this approach to any pathogen–antibiotic pair of interest, requiring only that an antibiotic elicit a differential transcriptional response in susceptible versus resistant isolates, a biological phenomenon that to date appears universal. For carbapenems, we incorporate simultaneous genotypic detection of key resistance determinants to improve accuracy of resistance detection and facilitate molecular epidemiology. Finally, we demonstrate GoPhAST-R directly on positive blood culture bottles, reporting phenotypic AST within hours of a positive culture. Together, this work establishes GoPhAST-R as an accurate, rapid approach to AST that leverages the advantages of both phenotypic and genotypic assays.

To identify transcripts that robustly distinguish susceptible and resistant bacteria after brief antibiotic exposure, we used RNA sequencing (RNA-seq) to compare transcriptional time courses of two susceptible and two resistant clinical isolates of *Klebsiella pneumoniae*, *Escherichia coli* and *Acinetobacter baumannii* (Supplementary Table 1) treated with meropenem (a carbapenem that inhibits cell wall biosynthesis), ciprofloxacin (a fluoroquinolone that targets DNA gyrase and topoisomerase) or gentamicin (an aminoglycoside that inhibits protein synthesis). Doses were chosen to match clinical breakpoint concentrations[26], defined by the Clinical and Laboratory Standards Institute (CLSI) as the antibiotic concentration above which resistant strains (that is, those at high risk of failing clinical therapy) can grow in broth microdilution assays. To enable these comparisons, we developed a library construction method optimized from RNAtag-seq[27] to include template switching, now termed RNAtag-seq_TS, to dramatically decrease cost and increase throughput (see Supplementary Methods). For each pathogen, each antibiotic elicited a transcriptional response within 30–60 min in susceptible but not resistant organisms (Fig. 1a and Extended Data Figs. 1a and 2).

To identify transcripts that best distinguish susceptible from resistant strains for each pathogen–antibiotic combination, we initially selected 60–100 candidate antibiotic-responsive transcripts from these RNA-seq datasets to evaluate in more clinical isolates. We used DESeq2 (ref. [28]) followed by Fisher's combined probability test to identify transcripts whose expression changed more on antibiotic treatment than under any phase of growth during the time course, thus enriching for genes directly affected by antibiotic exposure (see Supplementary Methods). Gene ontology enrichment analysis (Supplementary Table 2) revealed that meropenem affected lipopolysaccharide biosynthesis in both *Enterobacteriaceae* species, and induced a heat shock response in both *E. coli* and *Acinetobacter*. In all three species, ciprofloxacin induced the SOS response, while gentamicin induced the unfolded protein response and quinone binding. For normalization across samples, we also used DESeq2 to select 10–20 control transcripts for each pathogen–antibiotic pair that were most invariant to antibiotic treatment and growth phase (see Methods).

For each pathogen–antibiotic pair, we designed probesets for multiplexed detection of each candidate control and responsive transcript using NanoString, a simple, quantitative fluorescent hybridization platform that does not require nucleic acid purification or enzymology and thus works on crude lysates[17,29]. Each probeset comprised pairs of 50mer probes to conserved regions (see Methods) of the targeted transcripts (Supplementary Table 3). Using a protocol modified from the standard NanoString nCounter assay to accelerate detection (see Methods), we quantified these target transcripts in 18–24 diverse clinical isolates of each species collected from various geographic locations (Supplementary Table 1) and spanning the known phylogenetic landscape of each species (Extended Data Fig. 3). Because of a homology screening step in probe design (see Methods), each probe will uniquely hybridize to the target transcript from its cognate species, thereby enabling simultaneous species identification[17]. Normalized expression signatures of all responsive genes are shown as heatmaps (Extended Data Fig. 4) and summarized as one-dimensional projections (Extended Data Fig. 5).

To further test the generalizability of this approach, we repeated these steps from RNA-seq through NanoString detection of candidate responsive and control genes for two additional high-priority and frequently multidrug-resistant pathogens—*S. aureus*, a gram-positive, and *P. aeruginosa*, another gram-negative—each treated with a fluoroquinolone, levofloxacin (given its greater potency against gram-positives) and ciprofloxacin, respectively (Extended Data Fig. 6). Each robustly induced the SOS response (Supplementary Table 2) in susceptible but not resistant clinical isolates.

Importantly, expression signatures alone merely show that reliable differences occur in the transcriptional response in susceptible versus resistant organisms, while AST requires binary classification of a strain as susceptible or resistant. To address this general classification problem, we deployed machine learning algorithms (Extended Data Fig. 7, phase 1), first to identify the most informative transcripts, and then to use these select transcripts to classify unknown isolates. To avoid overtraining, we partitioned the tested strains into a training (derivation) cohort for both feature selection and classifier training, and a testing (validation) cohort as a naïve strain set for assessing classifier performance. We used reliefF to identify the ten transcripts whose normalized expression best distinguished susceptible from resistant organisms among the training cohort (Fig. 1b, Extended Data Figs. 1b and 6b and Supplementary Table 3). Although fewer than ten transcripts were required to robustly distinguish between the strains we have thus far tested, we opted to keep more genes in the refined signature to lessen the potential impact of unanticipated diversity in gene content, sequence or regulation among clinical isolates.

We next trained an ensemble classifier using a random forest model for binary classification of isolates in the derivation cohort based solely on these selected features, then tested this trained classifier on the validation cohort. Across all 11 bacteria–antibiotic combinations, 109 isolates were used as derivation strains for training and 108 isolates were tested as validation. The ensemble classifier correctly classified 100 of these 108 (93% categorical agreement; 95% confidence interval (95% CI), 87–96%), including 51 of 52 resistant isolates (1.9% very major error rate; 95% CI, 0.21–8.6%) and 35 of 38 susceptible isolates (7.9% major error rate; 95% CI, 2.3–20%), compared with standard broth microdilution (Fig. 1c, Extended Data Figs. 1c and 6c and Supplementary Table 4). Of note, these error rates are typically reported on a natural distribution of isolates. In contrast, for this study, we deliberately assembled a 'challenge set' of strains, intentionally overrepresented for isolates near the clinical breakpoints, which will artificially inflate all errors, since discrepant classifications are more common for strains with minimal inhibitory concentrations (MICs) near the breakpoint—both due to possible errors in the assay and to one-dilution errors inherent in the gold-standard broth microdilution assay[30]. Consistent with this, all major and very major errors in phase 1 testing involved strains less than or equal to two dilutions away from the clinical breakpoint (Fig. 1c and Extended Data Figs. 1c and 6c).

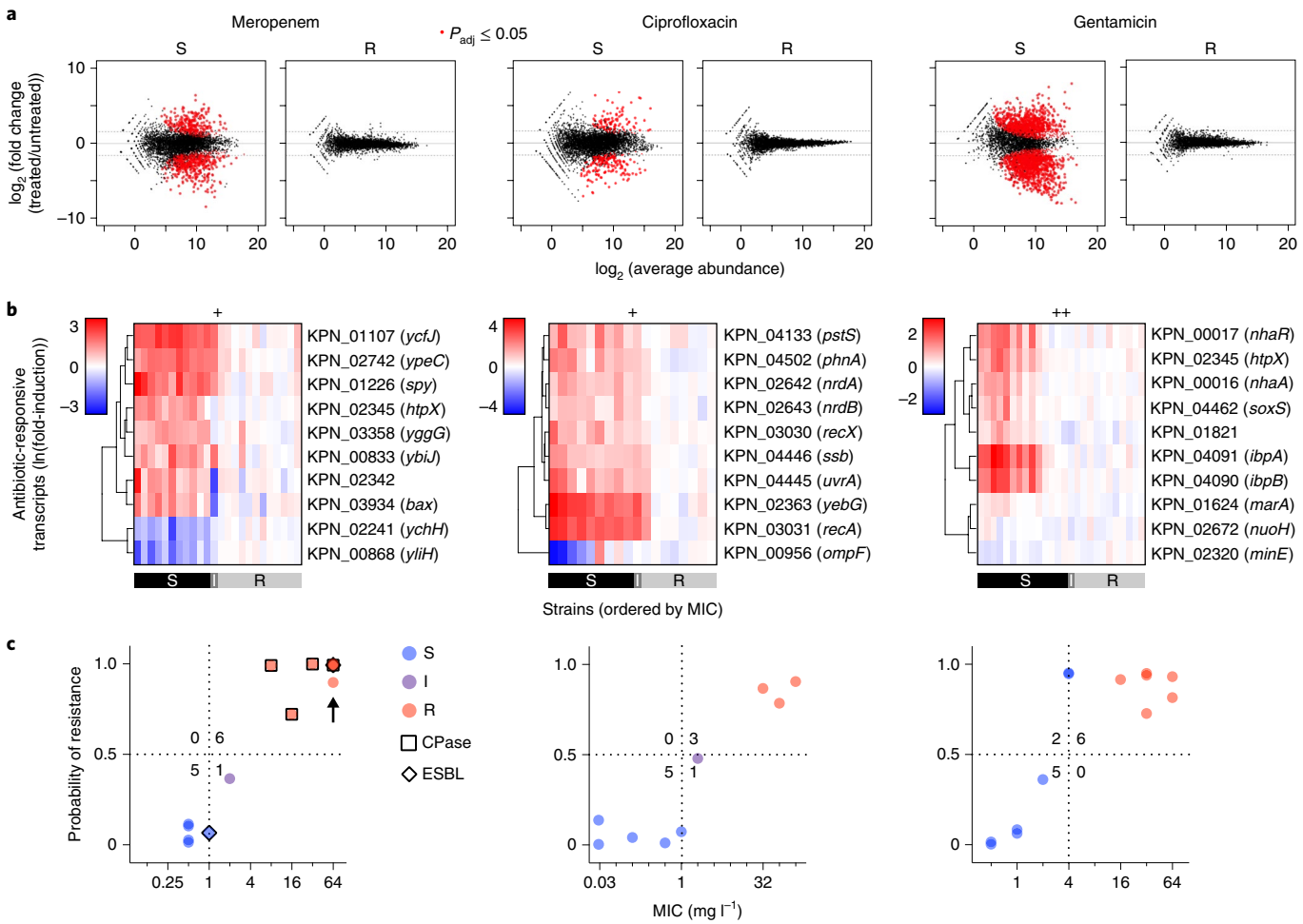


**Fig. 1 | Differential gene expression on antibiotic exposure distinguishes susceptible and resistant strains. a**, RNA-seq data from two susceptible (left panels) or two resistant (right panels) clinical isolates of *K. pneumoniae* treated with meropenem (60 min), ciprofloxacin (30 min) or gentamicin (60 min) at CLSI breakpoint concentrations are presented as MA plots. Statistical significance was determined by a two-sided Wald test with the Benjamini–Hochberg correction for multiple hypothesis testing, using the DESeq2 package[28]. **b**, Heatmaps of normalized, log-transformed fold-induction of top ten antibiotic-responsive transcripts from *K. pneumoniae* treated at CLSI breakpoint concentrations with meropenem (left, 24 independent clinical isolates), ciprofloxacin (center, 18 independent clinical isolates) or gentamicin (right, 26 independent clinical isolates). Gene identifiers are listed at right, along with gene names if available. CLSI classifications of each strain based on broth microdilution are shown below (S, susceptible; R, resistant; I, intermediate). +, strains with one-dilution errors in classification. **c**, GoPhAST-R predictions of probability of resistance from a random forest model trained on NanoString data from the derivation cohort and tested on the validation cohort (*y* axis) are compared with standard CLSI classification based on broth microdilution MIC (*x* axis) for *K. pneumoniae* isolates treated with meropenem, ciprofloxacin and gentamicin. Horizontal dashed lines indicate 50% probability of resistance. Vertical dashed lines indicate the CLSI breakpoint between susceptible and not susceptible (that is, intermediate/resistant). Numbers in each quadrant indicate concordant and discordant classifications between GoPhAST-R and broth microdilution. Carbapenemase (square outline) and select ESBL (diamond outline) gene content as detected by GoPhAST-R are also displayed on the meropenem plot. Arrow indicates a strain with high-level meropenem resistance, but no carbapenemase. CPase, carbapenemase; I, intermediate; $P_{adj}$, adjusted *P* value; R, resistant; S, susceptible.

To assess this approach to classification as it would be deployed on unknown isolates, and to further ensure against overtraining on the initial set of isolates, we performed a second, iterative round of training on all strains (from both derivation and validation cohorts) from phase 1. We then tested a new set of *K. pneumoniae* isolates treated with meropenem and ciprofloxacin (Extended Data Fig. 7, phase 2), this time measuring only the top ten selected responsive transcripts (as we envision for the ultimate assay), rather than the 60–100 transcripts measured in phase 1 (Extended Data Fig. 8a). Here, GoPhAST-R correctly classified 52 of 55 strains (95% categorical agreement; 95% CI, 86–98%), including all 25 resistant isolates (0% very major error rate; 95% CI, 0–9.5%) and 25 of 27 susceptible isolates (7.4% major error rate; 95% CI, 1.6–22%), compared with broth microdilution (Extended Data Fig. 8b). All three discrepant isolates were less than or equal to two dilutions from the breakpoint.

Three isolates classified as meropenem-resistant by GoPhAST-R but susceptible by broth microdilution exhibited a large inoculum effect[31]. These three isolates, a *K. pneumoniae* (BAA2524; Fig. 1b,c) and two *E. coli* (BAA2523 and AR0104; Extended Data Fig. 1b,c), all had MICs of 0.5–1 mg l$^{-1}$ on standard broth microdilution with an inoculum of $10^5$ colony-forming units (c.f.u.) ml$^{-1}$, but MICs of ≥32 mg l$^{-1}$ with an inoculum of $10^7$ c.f.u. ml$^{-1}$. Each of these strains carried a carbapenemase gene: BAA2523 and BAA2524 contained $bla_{OXA-48}$, and AR0104 contained $bla_{KPC-4}$, as has been reported for other such strains with large inoculum effects[32]. While the clinical consequences of such large inoculum effects are uncertain, they may portend clinical failure, particularly in the setting of carbapenemase production[22]; detection of this phenomenon is a known gap in standard broth microdilution assays[5,25,31]. GoPhAST-R classified these strains as phenotypically resistant, perhaps because the assay

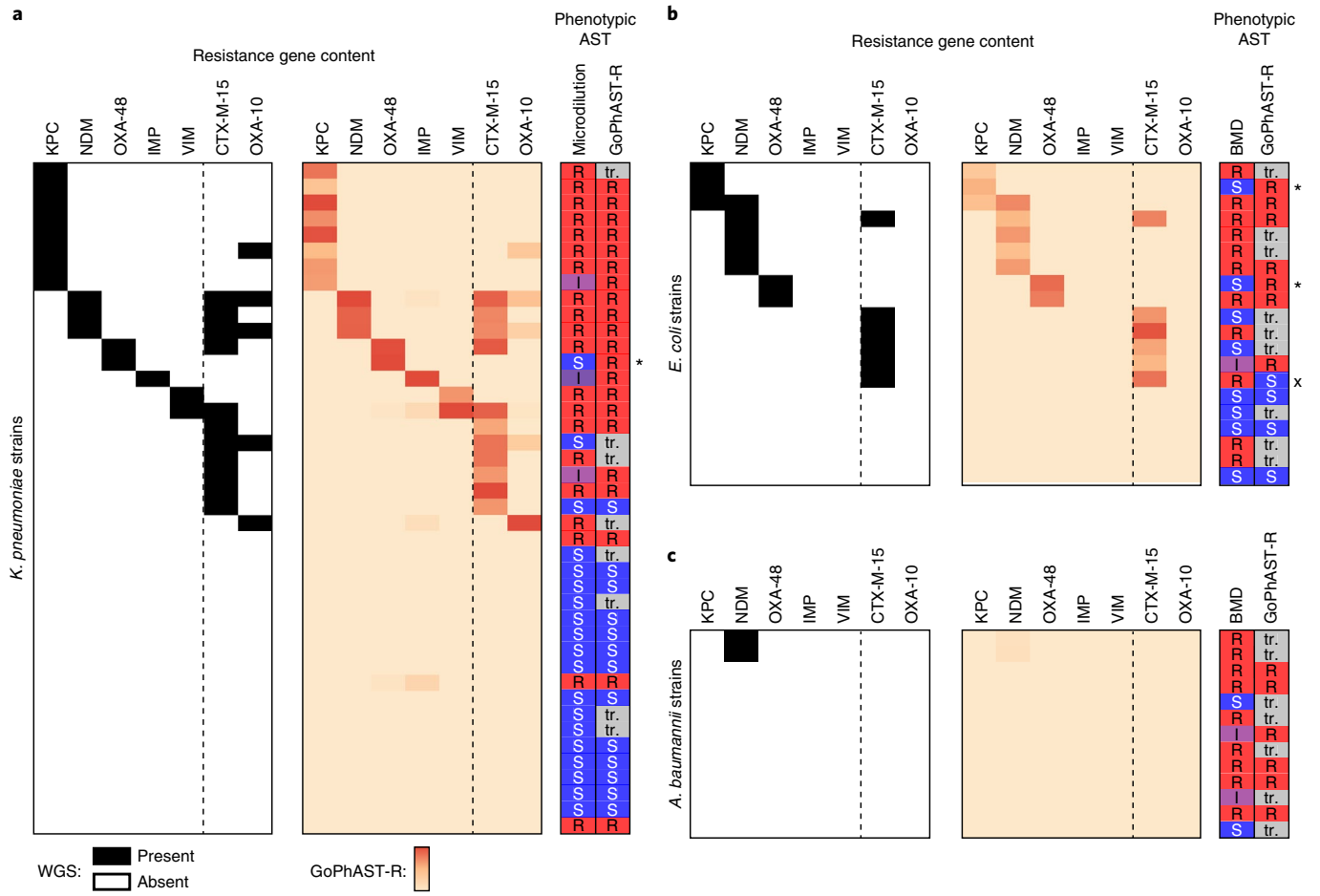


**Fig. 2 | GoPhAST-R detects carbapenemase and ESBL gene content from tested strains. a–c**, Known carbapenemase and select ESBL transcript content based on WGS data (left panels) are compared with heatmaps of GoPhAST-R results (right panels) for all *K. pneumoniae* (**a**), *E. coli* (**b**) and *A. baumannii* (**c**) isolates tested for meropenem susceptibility for which WGS data were available (42, 20 and 13 independent clinical isolates, respectively). Heatmap intensity reflects normalized, background-subtracted, log-transformed NanoString data from probes for the indicated gene families. Vertical dashed line separates carbapenemases (left) from ESBL genes (right). Phenotypic AST classification by broth microdilution (BMD) and GoPhAST-R is shown at right. tr., strain used in training cohort, thus not classified by GoPhAST-R; *strains with large inoculum effects in meropenem MIC; x, strain discordant by more than one dilution.

is performed at higher cell density (>$10^7$ c.f.u. $ml^{-1}$). Thus, the gold-standard method likely misclassified these isolates as susceptible, while GoPhAST-R correctly recognized their resistance.

Importantly, classifier performance was independent of resistance mechanism, as exemplified for meropenem resistance. In total, 22 of 47 meropenem-resistant isolates, including 7 of 22 *K. pneumoniae*, 4 of 12 *E. coli* and 11 of 13 *A. baumannii*, lacked carbapenemases (Supplementary Table 1), yet 46 of these 47 isolates were correctly recognized as resistant by GoPhAST-R. These results underscore the ability of GoPhAST-R to assess phenotypic resistance, agnostic to its genotypic basis.

GoPhAST-R can readily accommodate simultaneous profiling of additional transcripts, including genetic resistance determinants such as carbapenemases. Such genotypic information can complement GoPhAST-R's phenotype-based AST classification while providing valuable epidemiological data. For example, each of the three isolates with discrepant classifications and prominent inoculum effects carried a carbapenemase gene. Indeed, the most common known mechanism for carbapenem resistance among the *Enterobacteriaceae* involves acquisition of one of several carbapenemase genes[23], most commonly the KPC, NDM, OXA-48, IMP and VIM families[33]. We thus incorporated probes for these carbapenemases into the GoPhAST-R assay for meropenem AST, as well as two extended-spectrum beta-lactamase (ESBL) gene families that have been associated with carbapenem resistance when expressed in the context of porin loss-of-function, CTX-M-15 (ref. [34]) and OXA-10 (ref. [35]) (Supplementary Table 3).

GoPhAST-R correctly detected all 39 carbapenemase genes across 38 strains known to be present by WGS, including at least one member of each of the five targeted classes, and all 29 ESBL genes across 26 strains; no signal was detected in the 22 meropenem-resistant strains or the 38 susceptible isolates known to lack these gene families, across all three species (Fig. 2). This included detection of OXA-48 or KPC in the three cases of discrepant phenotypic AST classification and prominent inoculum effects, reinforcing GoPhAST-R's resistant phenotypic classification. Thus, in a single assay, GoPhAST-R can provide both phenotypic AST and genotypic information about resistance mechanism, which together result in the most accurate AST classification and valuable characterization of resistant isolates, including immediate recognition of unexplained resistance.

We previously demonstrated that a simulated positive blood culture bottle contains sufficient bacteria to permit mRNA detection by NanoString[36]. To demonstrate one valuable clinical application, we used GoPhAST-R to rapidly determine ciprofloxacin susceptibility in blood culture bottles that grew gram-negative rods from

the clinical microbiology laboratory at Massachusetts General Hospital (MGH). Ciprofloxacin was chosen because no rapid genotypic method exists for detection of fluoroquinolone resistance due to the diversity of genetic causes, and because the prevalence of fluoroquinolone resistance facilitated acquisition of both sensitive and resistant cases. Of six *E. coli* and two *K. pneumoniae* clinical positive blood cultures (Fig. 3), GoPhAST-R clearly distinguished three susceptible from three resistant *E. coli*; both *K. pneumoniae* species were susceptible. Given the relative scarcity of gentamicin and meropenem resistance at our institution, to test assay performance in this growth format, we generated simulated positive blood cultures by spiking in susceptible or resistant isolates of *K. pneumoniae* and *E. coli*. GoPhAST-R detected transcriptional signatures for each pathogen–antibiotic pair directly from these positive blood culture bottles, and blinded AST prediction using a random forest model and leave-one-out cross-validation correctly classified 71 of 72 blood cultures (99% categorical agreement with broth microdilution; 95% CI, 94–100%), including 31 of 31 resistant isolates (0% very major error rate; 95% CI, 0–7.7%) and 37 of 38 susceptible isolates (2.6% major error rate; 95% CI, 0.29–11%), compared with broth microdilution (Extended Data Fig. 9).

To decrease the time to answer, we deployed GoPhAST-R on a next-generation nucleic acid detection platform, NanoString Hyb & Seq (J.B., AGBT Precision Health 2017, unpublished abstract), whose accelerated detection technology enables AST in <4 h from the time a blood culture turns positive (Fig. 4a). Relative to the nCounter detection platform, Hyb & Seq (Fig. 4b) accelerates hybridization by using unlabeled reporter probes that are far smaller and thus equilibrate much faster than standard nCounter probes, which contain bulky fluorophores. Accelerated optical scanning rapidly quantifies these smaller reporter probes via sequential cycles of binding, detection and removal of complementary barcoded fluorophores (Fig. 4c and see Methods). On a prototype Hyb & Seq instrument, GoPhAST-R measured meropenem susceptibility signatures and carbapenemase content in <4 h (Fig. 4d). A head-to-head time trial on simulated blood culture bottles demonstrated GoPhAST-R results in <4 h from the time of culture positivity, compared with 28–40 h in the MGH clinical microbiology laboratory by standard methods (subculture followed by AST on a VITEK-2 instrument).

In summary, by quantifying a refined set of transcripts whose antibiotic-induced expression reflects susceptibility, GoPhAST-R provides a conceptually distinct approach to rapid phenotypic AST, agnostic to resistance mechanism and extendable to any pathogen and antibiotic class, while simultaneously providing select, complementary genotypic information. The machine learning approach to strain classification developed for GoPhAST-R provides actionable AST information in excellent categorical agreement with the gold-standard broth microdilution assay and should continue to improve in accuracy as it is trained on additional strains. Omitting three carbapenemase-producing strains with ambiguous and likely errant susceptible classification by the gold-standard assay, GoPhAST-R correctly classified 100 of 106 strains (94%) in phase 1, 52 of 54 strains (96%) in phase 2, and 71 of 72 (99%) simulated blood cultures, with eight of the nine discrepancies occurring on strains within two dilutions of the clinical breakpoint.

By integrating genotypic and phenotypic information in a single rapid multiplexed RNA detection assay, GoPhAST-R offers several advantages over the current gold standard that are unique among other rapid AST assays under development. First, as with other phenotypic assays, it determines susceptibility agnostic to mechanism of resistance, a clear advantage over genotypic AST assays. Second, combining genotypic and phenotypic information enhances AST accuracy over conventional growth-based methods, improving sensitivity of resistance detection in carbapenemase-producing *Enterobacteriaceae* that test susceptible by standard methods but may exhibit resistance on treatment[21,22,25]. Third, identification of

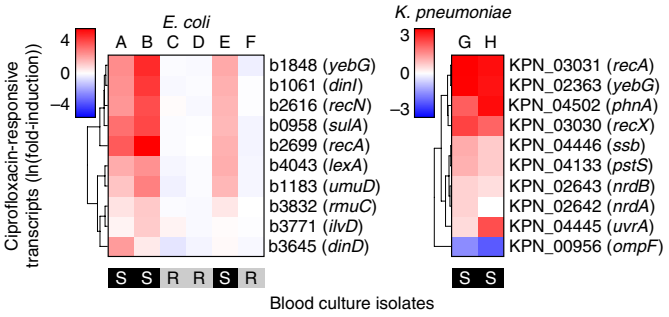


**Fig. 3 | GoPhAST-R detects antibiotic-responsive transcripts directly from positive blood culture bottles.** Heatmaps of normalized, log-transformed fold-induction of the top ten ciprofloxacin-responsive transcripts from eight positive blood culture bottles that grew either *E. coli* (six independent bottles, A–F) or *K. pneumoniae* (two independent bottles, G and H). CLSI classifications of isolates performed by the clinical microbiology laboratory, blinded until analysis was complete, are displayed below each heatmap.

carbapenem resistance determinants can inform antibiotic choice, as certain new beta-lactamase inhibitors such as avibactam or vaborbactam will overcome some classes of carbapenemases (for example, KPC) but not others (for example, metallo-beta-lactamases such as the NDM class)[37,38]. Solely phenotypic assays would require additional, serial testing to provide such guidance. Fourth, detecting resistance determinants together with a phenotypic assay enables molecular epidemiology for local, regional, national or global tracking of the emergence and spread of resistance, without requiring additional testing. We demonstrate this advantage for one major class of high-value resistance determinants, the carbapenemases; this combined approach can readily extend to other critical emerging resistance determinants such as *mcr* genes, plasmid-borne colistin resistance determinants recently found in *Enterobacteriaceae*[39] or key virulence factors such as *Shiga* toxin, in seamless conjunction with a phenotypic AST assay. Fifth, strains with unknown resistance mechanisms, such as CREs without carbapenemases (see Fig. 1 and Extended Data Fig. 8), can be immediately identified from a single assay and flagged for further study such as WGS if desired.

This work represents an important demonstration of this new approach to AST, enabling rapid, accurate classification across a genetically diverse sampling (Extended Data Fig. 2) of five high-priority pathogens and three major antibiotic classes. Still, further development will be needed for translation to clinical practice. With wider testing, while the specific classifiers will improve, the general strategy and approach remain valid. Indeed, the capacity to learn through iterative retraining is one of the strengths of this approach as it is used more broadly. Likewise, extending this assay to more pathogen–antibiotic pairs will be critical for widespread clinical utility. Fortunately, the experimental and computational approach described here allows rapid and conceptually straightforward extension to all pathogens and antibiotic classes, including those with new mechanisms of action and as-yet-unknown or newly emerging mechanisms of resistance. Underscoring the generalizability of this approach, we have generated preliminary RNA-seq data for 50 additional pathogen–antibiotic pairs, spanning gram-positive bacteria, gram-negative bacteria and mycobacteria, treated with bactericidal and bacteriostatic antibiotics, that demonstrate early differential transcriptional responses to antibiotics in all cases tested (R.P.B., P.M., S.S., J. Liu, L.W., R.F.R., M.M.P., J. Livny and D.T.H., unpublished results). Because GoPhAST-R is explicitly informed by clinical breakpoint concentrations, it leverages decades of earlier studies linking in vitro behavior to clinical outcomes[26], facilitating extension to new pathogens or antibiotics. GoPhAST-R cannot, however, overcome all limitations of current diagnostics, including

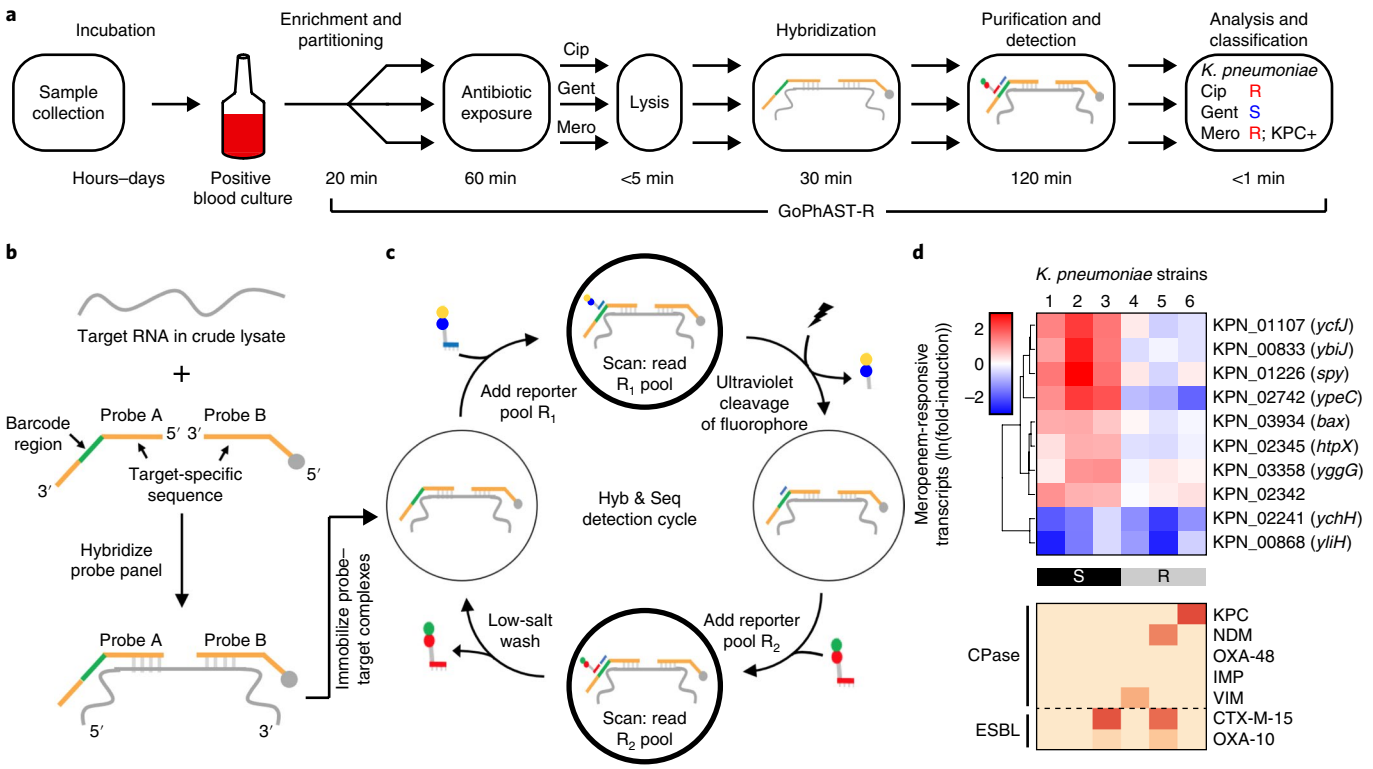


**Fig. 4 | GoPhAST-R workflow with the NanoString Hyb & Seq platform distinguishes phenotypically susceptible from resistant strains and detects genetic resistance determinants in <4 h. a**, The GoPhAST-R workflow on the Hyb & Seq detection platform begins once growth is detected in a blood culture bottle. Pathogen identification could either be done before this process, or in parallel by multiplexing mRNA targets from multiple organisms (see Supplementary Methods). **b**, Hyb & Seq hybridization scheme: probe pairs targeting each RNA transcript are hybridized in crude lysate. Each probe A contains a unique barcode sequence (green) for detection and a shared 3′ capture sequence; each probe B contains a biotin group (gray circle) for surface immobilization and a shared 5′ capture sequence. **c**, Hyb & Seq detection strategy: immobilized, purified ternary probe–target complexes undergo sequential cycles of multistep imaging for spatially resolved single-molecule detection. Each cycle consists of reporter probe binding and detection, ultraviolet cleavage, a second round of reporter probe binding and detection, and a low-salt wash to regenerate the unbound probe–target complex. Five Hyb & Seq cycles were used to generate the data shown. See Supplementary Methods for details. **d**, Pilot studies for accelerated meropenem susceptibility testing of six clinical *K. pneumoniae* isolates. Top: heatmaps of normalized, log-transformed fold-induction of top ten meropenem-responsive transcripts measured using this Hyb & Seq workflow, with strains arranged in order of MIC for each antibiotic. CLSI classifications are shown below. Bottom: heatmaps of normalized, background-subtracted, log-transformed NanoString data from carbapenemase (CPase) and select ESBL transcripts measured in the same Hyb & Seq assay. Cip, ciprofloxacin; Gent, gentamicin; Mero, meropenem.

an initial delay for blood culture, driven by the low abundance of bacteria, and thus bacterial mRNA, in the bloodstream of patients with infection. Still, considering the widespread adoption and clinical benefits[40] of rapid pathogen identification by matrix-associated laser desorption and ionization/time-of-flight (MALDI-TOF) mass spectrometry in 2 h from subcultured colonies streaked from blood culture bottles[40], this comparatively more informative AST assay directly from blood culture bottles in <4 h would be potentially transformative. We also anticipate the potential to expand GoPhAST-R to other clinical specimen types; some, such as urine, contain enough bacteria without culture to enable direct mRNA profiling[17]. Additionally, characterizing mixed populations of susceptible and resistant strains within an individual sample remains challenging for GoPhAST-R, which integrates transcription across bulk populations, just as it is for existing gold-standard methods that undergo a single-colony bottleneck during subculture. Finally, GoPhAST-R cannot completely overcome the challenge of identifying delayed inducible resistance, though this would be true for any rapid phenotypic test. In fact, GoPhAST-R may accurately identify at least some of these cases through simultaneous genotypic detection of induced resistance determinants, if known.

We have herein demonstrated the application of a next-generation nucleic acid detection platform that can return AST answers in <4 h. We have shown that the strategy is generalizable across a number of bacterial species and antibiotic classes, and will likely be widely applicable based on its conserved underlying biological principle. Notably, a reliable transcriptional signature of susceptibility is present in ≤1 h for each of these key antibiotic classes. Thus, as RNA detection methods become faster and more sensitive, GoPhAST-R has the potential for even faster phenotypic AST on timescales that can inform early antibiotic decisions and thus transform infectious disease practice.

## Online content

Any methods, additional references, Nature Research reporting summaries, source data, extended data, supplementary information, acknowledgements, peer review information; details of author contributions and competing interests; and statements of data and code availability are available at https://doi.org/10.1038/s41591-019-0650-9.

Received: 13 March 2019; Accepted: 11 October 2019;
Published online: 25 November 2019

## References

1. Fauci, A. S. & Morens, D. M. The perpetual challenge of infectious diseases. *N. Engl. J. Med.* **366**, 454–461 (2012).

2. *Antimicrobial Resistance: Global Report on Surveillance 2014* (World Health Organization, 2014).
3. Kumar, A. et al. Duration of hypotension before initiation of effective antimicrobial therapy is the critical determinant of survival in human septic shock. *Crit. Care Med.* **34**, 1589–1596 (2006).
4. Kadri, S. S. et al. Difficult-to-treat resistance in gram-negative bacteremia at 173 US hospitals: retrospective cohort analysis of prevalence, predictors, and outcome of resistance to all first-line agents. *Clin. Infect Dis.* **67**, 1803–1814 (2018).
5. Wiegand, I., Hilpert, K. & Hancock, R. E. Agar and broth dilution methods to determine the minimal inhibitory concentration (MIC) of antimicrobial substances. *Nat. Protoc.* **3**, 163–175 (2008).
6. Evans, S. R. et al. Rapid molecular diagnostics, antibiotic treatment decisions, and developing approaches to inform empiric therapy: PRIMERS I and II. *Clin. Infect Dis.* **62**, 181–189 (2016).
7. Arzanlou, M., Chai, W. C. & Venter, H. Intrinsic, adaptive and acquired antimicrobial resistance in Gram-negative bacteria. *Essays Biochem.* **61**, 49–59 (2017).
8. Cerqueira, G. C. et al. Multi-institute analysis of carbapenem resistance reveals remarkable diversity, unexplained mechanisms, and limited clonal outbreaks. *Proc. Natl Acad. Sci. USA* **114**, 1135–1140 (2017).
9. Milheirico, C., de Lencastre, H. & Tomasz, A. Full-genome sequencing identifies in the genetic background several determinants that modulate the resistance phenotype in methicillin-resistant *Staphylococcus aureus* strains carrying the novel mecC gene. *Antimicrob. Agents Chemother.* **61**, e02500-16 (2017).
10. Burnham, C. D., Leeds, J., Nordmann, P., O'Grady, J. & Patel, J. Diagnosing antimicrobial resistance. *Nat. Rev. Microbiol.* **15**, 697–703 (2017).
11. Consortium, C. R. et al. Prediction of susceptibility to first-line tuberculosis drugs by DNA sequencing. *N. Engl. J. Med.* **379**, 1403–1415 (2018).
12. Jia, B. et al. CARD 2017: expansion and model-centric curation of the comprehensive antibiotic resistance database. *Nucleic Acids Res.* **45**, D566–D573 (2017).
13. Bhattacharyya, R. P., Grad, Y. H. & Hung, D. T. in *Harrison's Principles of Internal Medicine* (eds J. L. Jameson et al.) Ch. 474 (McGraw-Hill Education, 2018).
14. Ellington, M. J. et al. The role of whole genome sequencing in antimicrobial susceptibility testing of bacteria: report from the EUCAST Subcommittee. *Clin. Microbiol. Infect.* **23**, 2–22 (2017).
15. Charnot-Katsikas, A. et al. Use of the accelerate pheno system for identification and antimicrobial susceptibility testing of pathogens in positive blood cultures and impact on time to results and workflow. *J. Clin. Microbiol.* **56**, e01166-17 (2018).
16. Cermak, N. et al. High-throughput measurement of single-cell growth rates using serial microfluidic mass sensor arrays. *Nat. Biotechnol.* **34**, 1052–1059 (2016).
17. Barczak, A. K. et al. RNA signatures allow rapid identification of pathogens and antibiotic susceptibilities. *Proc. Natl Acad. Sci. USA* **109**, 6217–6222 (2012).
18. Quach, D. T., Sakoulas, G., Nizet, V., Pogliano, J. & Pogliano, K. Bacterial cytological profiling (BCP) as a rapid and accurate antimicrobial susceptibility testing method for *Staphylococcus aureus*. *EBioMedicine* **4**, 95–103 (2016).
19. van Belkum, A., Welker, M., Pincus, D., Charrier, J. P. & Girard, V. Matrix-assisted laser desorption ionization time-of-flight mass spectrometry in clinical microbiology: what are the current issues? *Ann. Lab. Med.* **37**, 475–483 (2017).
20. Bonomo, R. A. et al. Carbapenemase-producing organisms: a global scourge. *Clin. Infect. Dis.* **66**, 1290–1297 (2018).
21. Lutgring, J. D. & Limbago, B. M. The problem of carbapenemase-producing-carbapenem-resistant-*Enterobacteriaceae* detection. *J. Clin. Microbiol.* **54**, 529–534 (2016).
22. Weisenberg, S. A., Morgan, D. J., Espinal-Witter, R. & Larone, D. H. Clinical outcomes of patients with *Klebsiella pneumoniae* carbapenemase-producing *K. pneumoniae* after treatment with imipenem or meropenem. *Diagn. Microbiol. Infect. Dis.* **64**, 233–235 (2009).
23. Woodworth, K. R. et al. Vital signs: containment of novel multidrug-resistant organisms and resistance mechanisms—United States, 2006–2017. *MMWR Morb. Mortal. Wkly Rep.* **67**, 396–401 (2018).
24. McMullen, A. R., Yarbrough, M. L., Wallace, M. A., Shupe, A. & Burnham, C. D. Evaluation of genotypic and phenotypic methods to detect carbapenemase production in gram-negative bacilli. *Clin. Chem.* **63**, 723–730 (2017).
25. Humphries, R. M. CIM City: the game continues for a better carbapenemase test. *J. Clin. Microbiol.* **57**, e00353-19 (2019).
26. *M100: Performance Standards for Antimicrobial Susceptibility Testing* 28th edn (Clinical and Laboratory Standards Institute, 2018).
27. Shishkin, A. A. et al. Simultaneous generation of many RNA-seq libraries in a single reaction. *Nat. Methods* **12**, 323–325 (2015).
28. Love, M. I., Huber, W. & Anders, S. Moderated estimation of fold change and dispersion for RNA-seq data with DESeq2. *Genome Biol.* **15**, 550 (2014).
29. Geiss, G. K. et al. Direct multiplexed measurement of gene expression with color-coded probe pairs. *Nat. Biotechnol.* **26**, 317–325 (2008).
30. *M07: Methods for Dilution Antimicrobial Susceptibility Tests for Bacteria that Grow Aerobically* 11th edn (Clinical and Laboratory Standards Institute, 2018).
31. Smith, K. P. & Kirby, J. E. The inoculum effect in the era of multidrug resistance: minor differences in inoculum have dramatic effect on MIC determination. *Antimicrob. Agents Chemother.* **62**, e00433-18 (2018).
32. Adler, A., Ben-Dalak, M., Chmelnitsky, I. & Carmeli, Y. Effect of resistance mechanisms on the inoculum effect of carbapenem in *Klebsiella pneumoniae* isolates with borderline carbapenem resistance. *Antimicrob. Agents Chemother.* **59**, 5014–5017 (2015).
33. Nordmann, P., Dortet, L. & Poirel, L. Carbapenem resistance in *Enterobacteriaceae*: here is the storm! *Trends Mol. Med.* **18**, 263–272 (2012).
34. Cubero, M. et al. Carbapenem-resistant and carbapenem-susceptible isogenic isolates of *Klebsiella pneumoniae* ST101 causing infection in a tertiary hospital. *BMC Microbiol.* **15**, 177 (2015).
35. Ma, P., Laibinis, H. H., Ernst, C. M. & Hung, D. T. Carbapenem resistance caused by high-level expression of OXA-663 beta-lactamase in an OmpK36-deficient *Klebsiella pneumoniae* clinical isolate. *Antimicrob. Agents Chemother.* **62**, e01281-18 (2018).
36. Hou, H. W., Bhattacharyya, R. P., Hung, D. T. & Han, J. Direct detection and drug-resistance profiling of bacteremias using inertial microfluidics. *Lab Chip* **15**, 2297–2307 (2015).
37. Lomovskaya, O. et al. Vaborbactam: Spectrum of beta-lactamase inhibition and impact of resistance mechanisms on activity in *Enterobacteriaceae*. *Antimicrob. Agents Chemother.* **61**, e01443-17 (2017).
38. Marshall, S. et al. Can ceftazidime-avibactam and aztreonam overcome beta-lactam resistance conferred by metallo-beta-lactamases in *Enterobacteriaceae*? *Antimicrob. Agents Chemother.* **61**, e02243-16 (2017).
39. Caniaux, I., van Belkum, A., Zambardi, G., Poirel, L. & Gros, M. F. MCR: modern colistin resistance. *Eur. J. Clin. Microbiol. Infect. Dis.* **36**, 415–420 (2017).
40. Florio, W., Tavanti, A., Barnini, S., Ghelardi, E. & Lupetti, A. Recent advances and ongoing challenges in the diagnosis of microbial infections by MALDI-TOF mass spectrometry. *Front. Microbiol.* **9**, 1097 (2018).

## Methods

**Strain acquisition and characterization.** All strains in this study (Supplementary Table 1) were obtained from clinical or reference microbiological laboratories, including both local hospitals and MDRO strain collections from the Centers for Disease Control Antibiotic Resistance Isolate Bank (https://wwwn.cdc.gov/ARIsolateBank/) and the New York State Department of Health. MICs reported from those laboratories were validated by standard broth microdilution assays[5] in Mueller–Hinton broth (Difco); any discrepancies of >1 doubling from reported values were resolved by repeating in triplicate. The Partners Health Care Institutional Review Board (IRB) approved strain collection under protocol 2015P002215 with waiver of patient consent, since bacterial isolates were obtained from clinical microbiology laboratories without any human material. Strains for which WGS data were available at the National Center for Biotechnology Information were visualized using the Interactive Tree of Life[41].

**RNA-seq experimental conditions.** For each bacteria–antibiotic pair, selected independent clinical isolates (Supplementary Table 1), two susceptible and two resistant, were grown at 37°C in Mueller–Hinton broth to early logarithmic phase, then treated with the relevant antibiotic at breakpoint concentrations set by the CLSI[26]: 2 mg l$^{-1}$ for meropenem, 1 mg l$^{-1}$ for ciprofloxacin and 4 mg l$^{-1}$ for gentamicin. Total RNA was harvested from paired treated and untreated samples at 0, 10, 30 and 60 min. cDNA libraries were made using a variant of the RNAtag-seq protocol we previously described[27] and sequenced on either an Illumina HiSeq or NextSeq. Sequencing reads were aligned using the Burrows–Wheeler Aligner (BWA)[42] and tabulated as previously described[27]. See the Supplementary Methods for further details.

**Differential gene expression analysis and selection of responsive and control transcripts.** Differentially expressed genes were determined using the DESeq2 package[28], comparing treated versus untreated samples at each timepoint using a two-sided Wald test with the Benjamini–Hochberg correction for multiple hypothesis testing. Fisher's combined probability test was used to select only those genes whose expression after antibiotic treatment is statistically distinguishable from its expression at any timepoint in the untreated samples. Gene ontology terms were assigned using blast2GO (ref. [43]) (v.1.4.4), with hypergeometric testing for enrichment. For each pathogen–antibiotic pair, the fold-change threshold in DESeq2 used to test statistical significance was increased to select 60–100 antibiotic-responsive transcripts with maximal stringency, a number readily accommodated by the NanoString assay format. Control transcripts were also determined with DESeq2 using an inverted hypothesis test as described[28] to select genes whose expression we expect to be unaffected by antibiotic exposure or growth in both susceptible and resistant isolates, at all timepoints and treatment conditions. As with responsive genes, the fold-change threshold was varied to select the top 10–20 control transcripts. The resulting control and responsive gene lists for each pathogen–antibiotic pair, and the fold-change thresholds used to generate them, are shown in Supplementary Table 3. See the Supplementary Methods for further details.

**Targeted transcriptional response to antibiotic exposure.** After using BLASTn to identify regions of targeted transcripts with maximal conservation across all RefSeq genomes from that species (see Supplementary Methods), NanoString probes were designed per the manufacturer's standard process[29] to these conserved regions. Strains treated with antibiotic at the CLSI breakpoint concentration, and untreated controls, were lysed via bead-beating at the desired timepoint. The resulting crude lysates were used as input for standard NanoString assays, which were performed on the nCounter Sprint platform with variations on the manufacturer's protocol to enhance speed, detailed in the Supplementary Methods. Raw counts for each target were extracted and processed as described in the Supplementary Methods. Briefly, for each sample, each responsive gene was normalized by control gene expression as a proxy for cell loading using a variation on the geNorm algorithm[44], then converted to fold-induction in treated compared with untreated strains. Pilot NanoString Hyb & Seq assays (Fig. 4) were performed on a prototype Hyb & Seq instrument at NanoString, with 20 min hybridization time and five imaging cycles to detect hybridization probes with two-segment, 10-plex barcodes. See the Supplementary Methods for more details.

**Machine learning: feature selection and susceptibility classification.** For each pathogen–antibiotic pair, we first partitioned the normalized data, grouping half of the strains into a derivation cohort on which we trained our algorithm, and reserving the other half for validation (Extended Data Fig. 5), ensuring equivalent representation of susceptible and resistant isolates in each cohort. For comparison of GoPhAST-R classifications with gold-standard results, confidence intervals for accuracy estimates were calculated using Jeffrey's interval[45].

In phase 1, implemented for all pathogen–antibiotic pairs, normalized fold-induction data of responsive genes from strains in the training cohort, along with CLSI susceptibility classification for each training strain, were input to the ReliefF algorithm[46] using the CORElearn package (v.1.52.0) to rank the top ten responsive transcripts that best distinguished susceptible from resistant strains. These ten features were then used to train a random forest classifier[47] using the caret package (v.6.0-78) in R (v.3.3.3) on the same training strains. Performance of this classifier was then assessed on the testing cohort, to which the classifier had yet to be exposed.

In phase 2, implemented for *K. pneumoniae* + meropenem and ciprofloxacin, all 18–24 strains from phase 1 were combined into a single, larger training set. For each antibiotic, ReliefF was again used to select the ten most informative responsive transcripts, which were then used to train a random forest classifier on the same larger training set. Transcriptional data were then collected on a test set of 25–30 new strains using a trimmed NanoString nCounter Elements probeset containing only probes for these ten selected transcripts, plus 8–13 control probes. Susceptibility of each strain in this test set was predicted using the trained classifier. See the Supplementary Methods for further details on machine learning strategy and implementation.

For classification of simulated blood cultures, NanoString data were collected for the top ten transcripts (selected in phase 1) from 12 strains for each pathogen–antibiotic pair, and analyzed using a leave-one-out cross-validation approach[48], training on 11 strains and classifying the 12th, then repeating with each strain omitted once from training and used for prediction.

**Blood culture processing.** Under Partners Health Care IRB 2015P002215, bacteria were isolated from real or simulated blood cultures in the MGH clinical microbiology laboratory, isolated by differential centrifugation, resuspended in Mueller–Hinton broth and immediately split for treatment with the indicated antibiotics. Lysis and targeted RNA detection were performed as described in "Targeted transcriptional response to antibiotic exposure." Specimens were blinded until all data acquisition and analysis was complete. See the Supplementary Methods for more detail. As approved by Partners IRB, samples were collected under waiver of patient consent due to experimental focus only on the bacterial isolates, not the patients from which they were derived.

**Reporting Summary.** Further information on research design is available in the Nature Research Reporting Summary linked to this article.

## Data availability

All RNA-seq data generated and analyzed for this study, supporting the analyses in Fig. 1 and Extended Data Figs. 1, 2 and 5, have been deposited as aligned bam files in the NCBI Sequencing Read Archive under study ID PRJNA518730. All other datasets generated during the current study, including raw and processed NanoString data, are available from the corresponding author on reasonable request.

## Code availability

Custom scripts for transcript selection from RNA-seq data are available at https://github.com/broadinstitute/GeneSelection/. Custom scripts for feature selection and strain classification from NanoString data are available at https://github.com/broadinstitute/DecisionAnalysis/. See the Nature Research Reporting Summary for additional detail.

## References

41. Letunic, I. & Bork, P. Interactive tree of life (iTOL) v4: recent updates and new developments. *Nucleic Acids Res.* **47**, W256–W259 (2019).
42. Li, H. & Durbin, R. Fast and accurate short read alignment with Burrows–Wheeler transform. *Bioinformatics* **25**, 1754–1760 (2009).
43. Gotz, S. et al. High-throughput functional annotation and data mining with the Blast2GO suite. *Nucleic Acids Res.* **36**, 3420–3435 (2008).
44. Vandesompele, J. et al. Accurate normalization of real-time quantitative RT-PCR data by geometric averaging of multiple internal control genes. *Genome Biol.* **3**, RESEARCH0034 (2002).
45. Brown, L. D., Cai, T. T. & DasGupta, A. Interval estimation for a binomial proportion. *Statist. Sci.* **16**, 101–133 (2001).
46. Robnik-Šikonja, M. & Kononenko, I. Theoretical and empirical analysis of ReliefF and RReliefF. *Mach. Learn.* **53**, 23–69 (2003).
47. Liaw, A. & Wiener, M. Classification and regression by randomForest. *R News* **2**, 18–22 (2002).
48. Efron, B. & Gong, G. A leisurely look at the bootstrap, the jackknife, and cross-validation. *Am. Stat.* **37**, 36–48 (1983).

## Acknowledgements

We thank T. Abeel for valuable early discussions about the approach to machine learning for feature selection and strain classification; E. Lander, B. Birren, C. Nusbaum and C. Russ for input on RNA-seq experiments and overall strategy; and G. Giannoukos and D. Ciulla for valuable contributions to RNA-seq methods development. This publication was supported in part by the National Institute of Allergy and Infectious Diseases of the National Institutes of Health (award nos. 1R01AI117043-05 to D.T.H. and 1K08AI119157-04 to R.P.B., and contract no. HHSN272200900018C). The content is solely the responsibility of the authors and does not necessarily represent the official views of the National Institutes of Health.

## Author contributions

R.P.B., J. Livny and D.T.H. conceived of the approach and designed experiments. R.P.B., S.S.S., J. Liu, R.F.R. and M.M.P. designed and executed the RNA-seq experiments. R.P.B., N.B., R.Y., N.S. and J. Livny planned and implemented the RNA-seq analysis, transcript selection and strain classification. R.P.B. analyzed strain phylogenies. R.P.B., P.M., G.C.C., A.P., A.M.E., J. Livny and D.T.H. planned and implemented the strategy for carbapenemase and ESBL gene detection. R.P.B., S.S.S., J. Liu and L.L.H. executed the NanoString experiments. R.P.B., J.S., V.M.P., L.L.H. and L.A.C. designed and executed clinical sample collection and processing for real and simulated blood cultures. E.N., K.A.M. and J.T. assisted with experimental design and sample acquisition for genotypic and phenotypic analysis of carbapenem-resistant clinical isolates. L.W., R.K., R.B. and J.B. designed and implemented the Hyb & Seq experiments. R.P.B. and D.T.H. primarily drafted the manuscript, with extensive input from J. Livny. All authors have read and approved the manuscript.

## Competing interests

R.P.B., P.M., J. Livny and D.T.H. are co-inventors on subject matter in US provisional application No. 62/723,417 filed by the Broad Institute directed to RNA signatures for AST, as described in this manuscript. L.W., R.B., R.K. and J.B. are employees at NanoString, Inc., the company that manufactures the RNA detection platforms used in this manuscript. NanoString, Inc. has licensed the intellectual property for RNA-based AST from the Broad Institute. V.M.P. received research funds from SeLux Diagnostics, Inc. for work on an unrelated project.

## Additional information

**Extended data** is available for this paper at https://doi.org/10.1038/s41591-019-0650-9.

**Supplementary information** is available for this paper at https://doi.org/10.1038/s41591-019-0650-9.

**Correspondence and requests for materials** should be addressed to D.T.H.

**Peer review information** Alison Farrell was the primary editor on this article and managed its editorial process and peer review in collaboration with the rest of the editorial team.

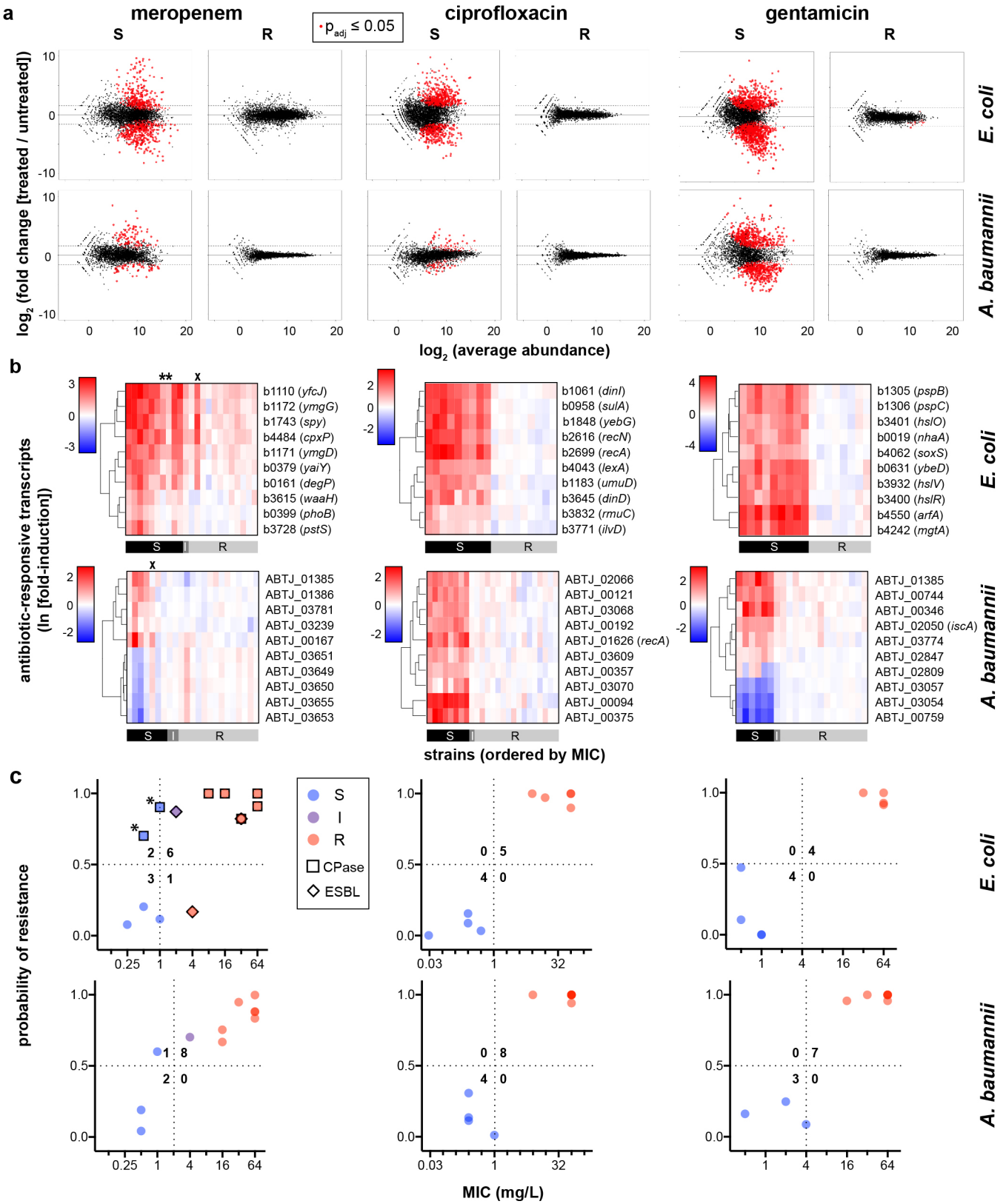


**Extended Data Fig. 1 | See next page for caption.**

**Extended Data Fig. 1 | Differential gene expression upon antibiotic exposure distinguishes susceptible and resistant strains.** (a) RNA-Seq data from two susceptible (left panels) or two resistant (right panels) clinical isolates of E. coli or A. baumannii treated with meropenem (60 min), ciprofloxacin (30 min), or gentamicin (60 min) at CLSI breakpoint concentrations are presented as MA plots. Statistical significance was determined by a two-sided Wald test with the Benjamini-Hochberg correction for multiple hypothesis testing, using the DESeq2 package[28]. (b) Heatmaps of normalized, log-transformed fold-induction of top 10 antibiotic-responsive transcripts from 24 clinical isolates of E. coli or A. baumannii treated at CLSI breakpoint concentrations with meropenem, ciprofloxacin, or gentamicin. Gene identifiers are listed at right, along with gene names if available. CLSI classifications of each strain based on broth microdilution are shown below. * = strains with large inoculum effects in meropenem MIC; x = strains discordant by more than one dilution. (c) GoPhAST-R predictions of probability of resistance from a random forest model trained on NanoString data from the derivation cohort and tested on the validation cohort (y-axis) are compared with standard CLSI classification based on broth microdilution MIC (x-axis) for E. coli (top) or A. baumannii isolates treated with meropenem, ciprofloxacin, and gentamicin. Horizontal dashed lines indicate 50% probability of resistance. Vertical dashed lines indicate the CLSI breakpoint between susceptible and not susceptible (that is intermediate/resistant). Numbers in each quadrant indicate concordant and discordant classifications between GoPhAST-R and broth microdilution. Carbapenemase (square outline) and select ESBL (diamond outline) gene content as detected by GoPhAST-R are also displayed on the meropenem plot.

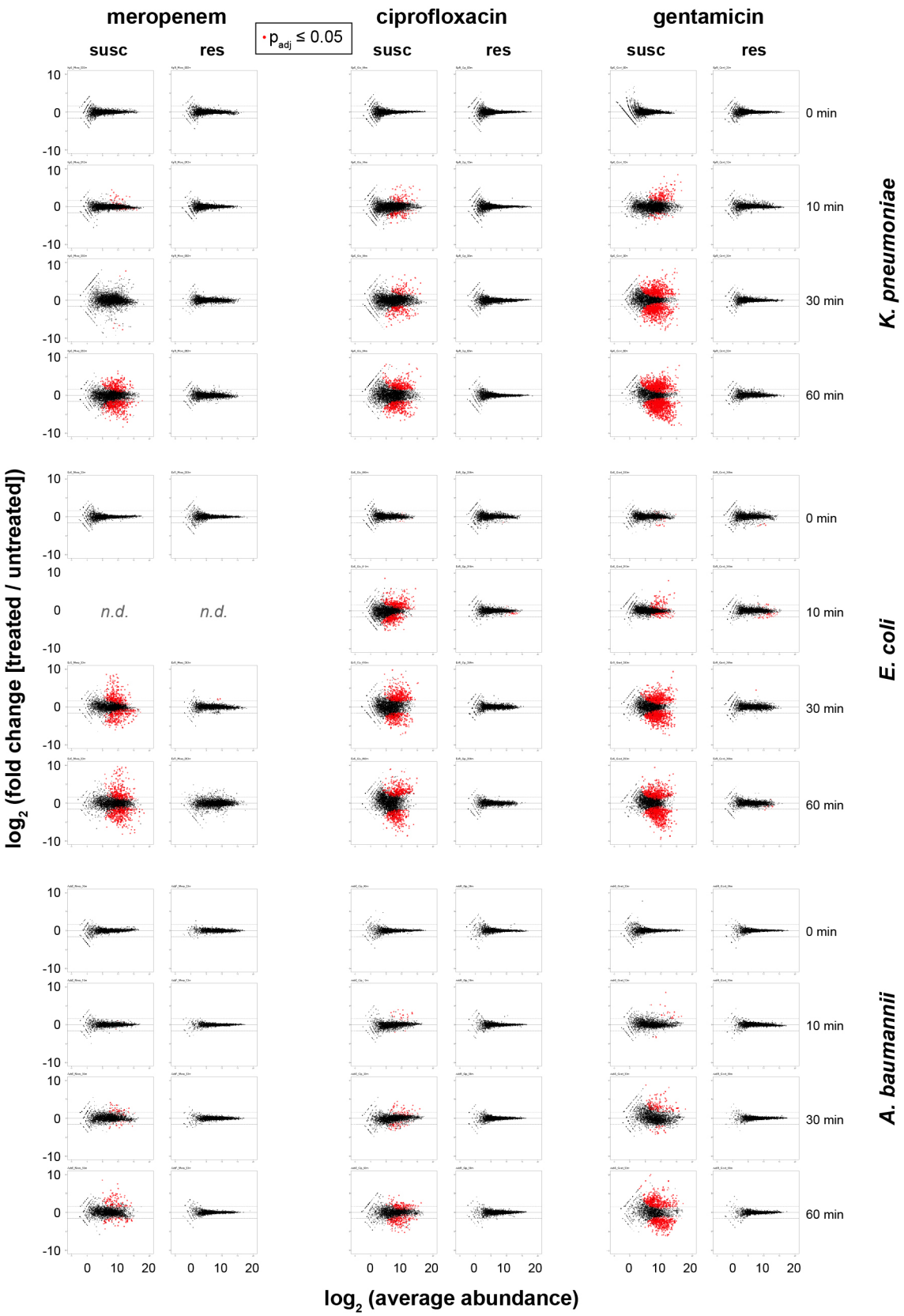


**Extended Data Fig. 2 | Timecourse of RNA-Seq data upon antibiotic exposure reveals differential gene expression between susceptible and resistant clinical isolates.** Susceptible (left panels) or resistant (right panels) clinical isolates of K. pneumoniae, E. coli, or A. baumannii treated with meropenem, ciprofloxacin, or gentamicin at CLSI breakpoint concentrations for the indicated times. Data are presented as MA plots, Statistical significance was determined by a two-sided Wald test with the Benjamini-Hochberg correction for multiple hypothesis testing, using the DESeq2 package[28].

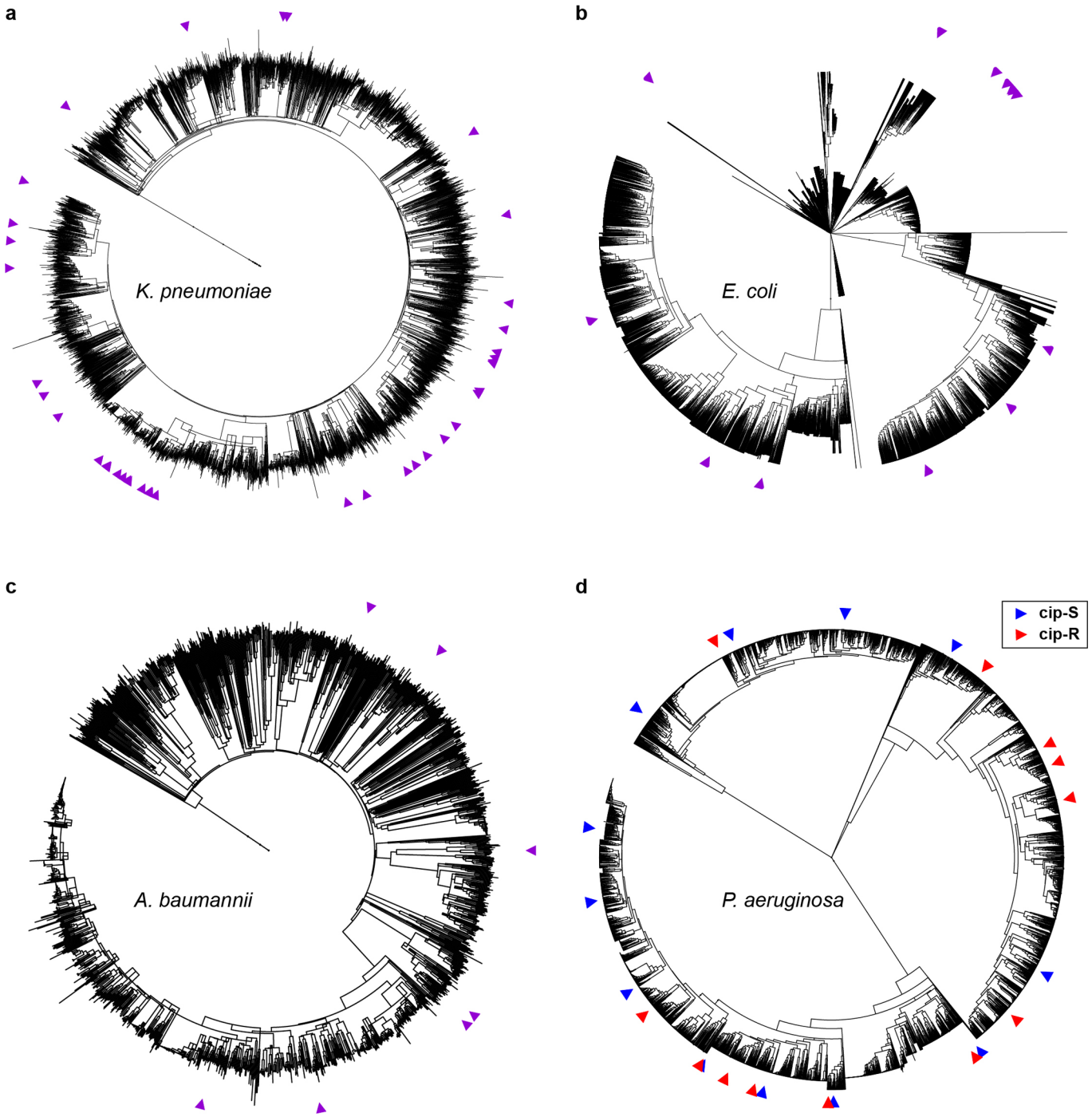


**Extended Data Fig. 3 | Phylogenetic trees highlight the diversity of strains used in this study.** Phylogenetic trees of all sequenced isolates deposited in NCBI for (a) K. pneumoniae, (b) E. coli, (c) A. baumannii, and (d) P. aeruginosa, with all sequenced isolates used in this study indicated by colored arrowheads around the periphery. See Supplementary Methods for details.

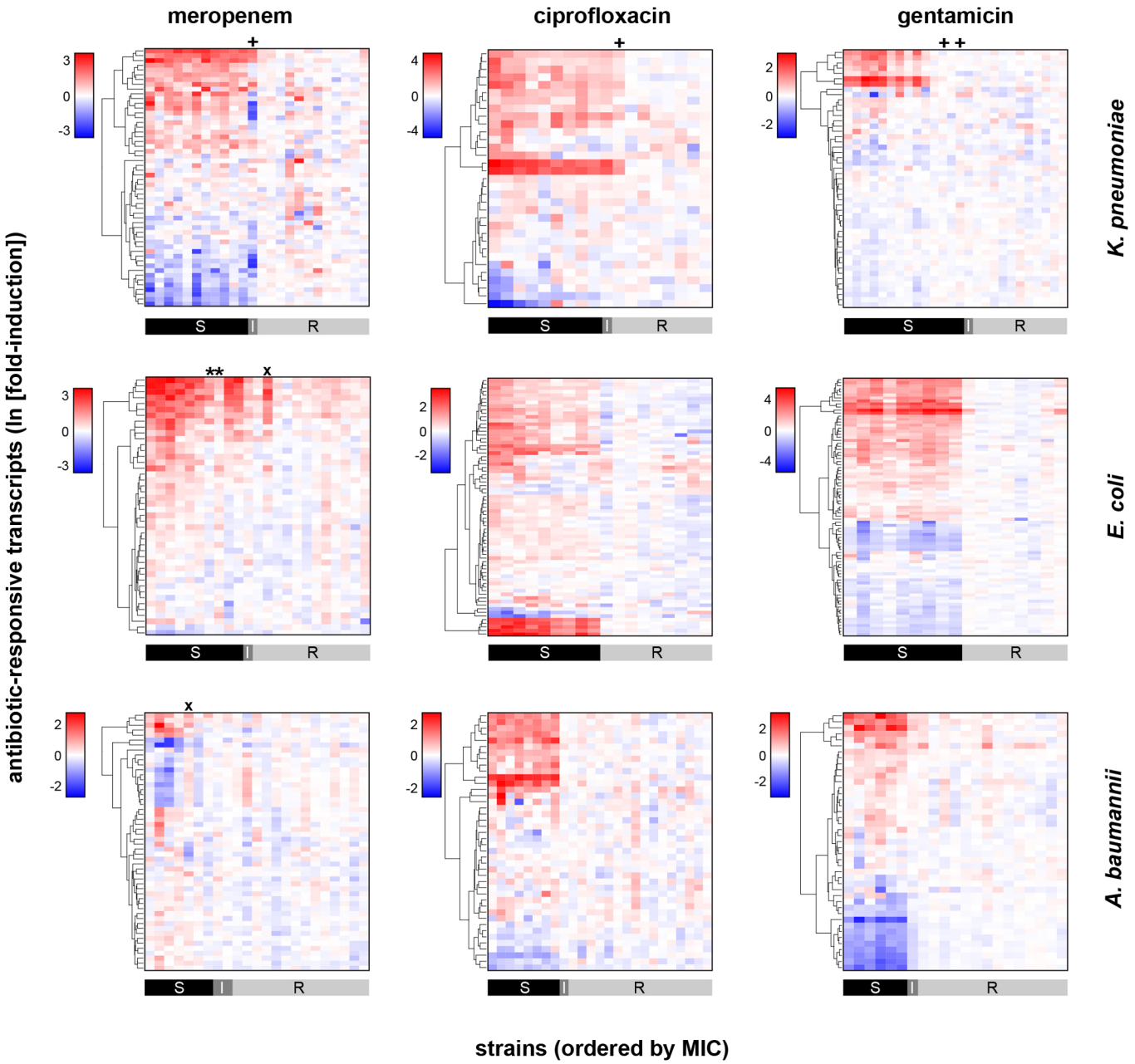


**Extended Data Fig. 4 | NanoString data from dozens of antibiotic-responsive genes distinguish susceptible from resistant isolates.** Heatmaps of normalized, log-transformed fold-induction of antibiotic-responsive transcripts from clinical isolates of *K. pneumoniae* (24, 18, and 26 independent clinical isolates for the three antibiotics, respectively), *E. coli* (24 independent clinical isolates for each antibiotic), or *A. baumannii* (24 clinical isolates for each antibiotic) treated at CLSI breakpoint concentrations with meropenem, ciprofloxacin, or gentamicin. CLSI classifications are shown below. All antibiotic-responsive transcripts chosen as described from RNA-Seq data are shown here; the subset of these chosen by reliefF as the 10 most discriminating transcripts are shown in Fig. 1b or Supplemental Fig. 1b. * = strains with large inoculum effects in meropenem MIC; + = one-dilution errors; x = strains discordant by more than one dilution.

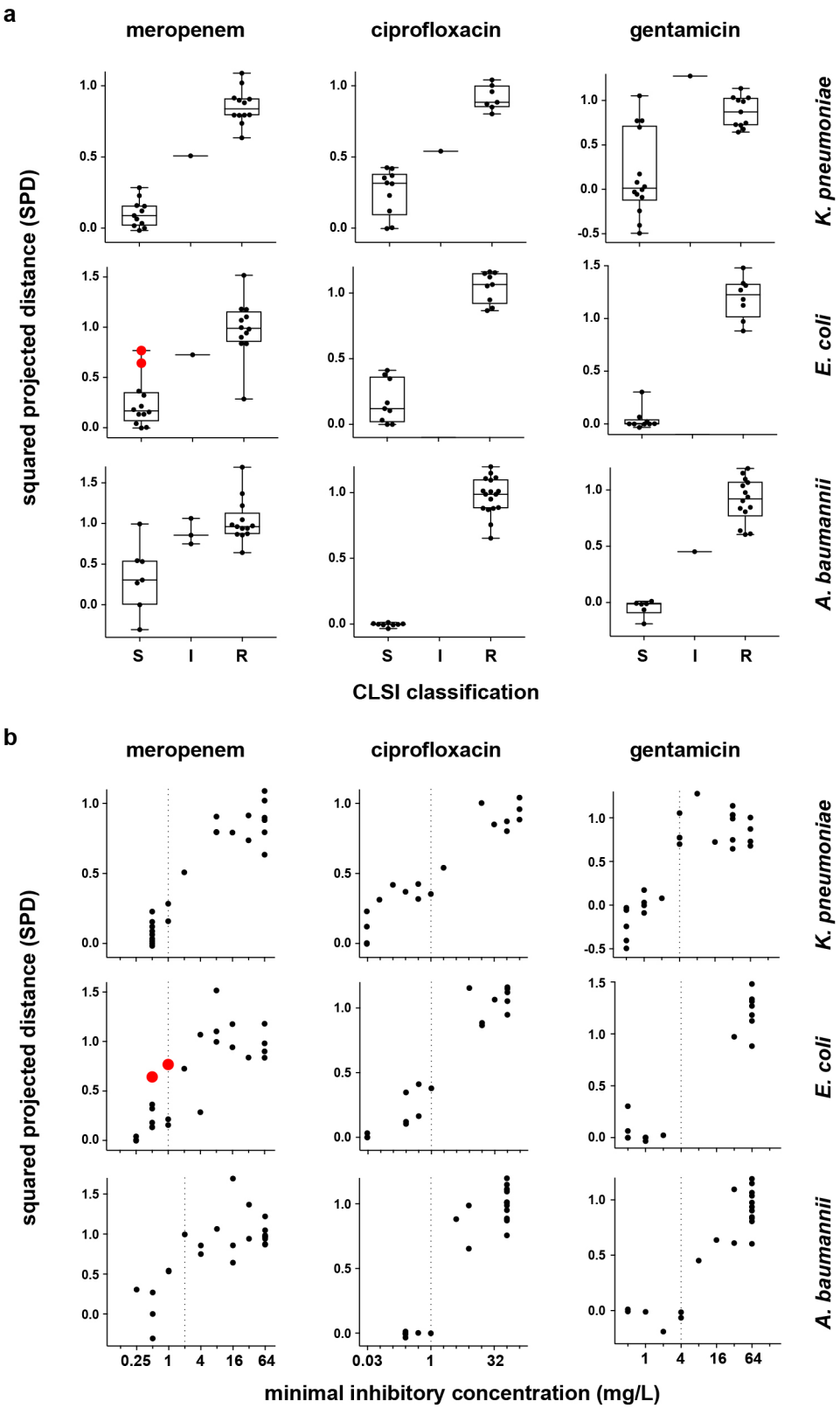


**Extended Data Fig. 5 |** See next page for caption.

**Extended Data Fig. 5 | One-dimensional projection of NanoString data distinguishes susceptible from resistant isolates and reflects MIC.** (a) Phase 1 NanoString data from Supplemental Fig. 2 (that is, normalized, log-transformed fold-induction for each responsive transcript), analyzed as described to generate squared projected distance (SPD) metrics (y-axes) for each strain (see Supplementary Methods), are binned by CLSI classifications (x-axes), for clinical isolates of *K. pneumoniae* (24, 18, and 26 independent clinical isolates for the three antibiotics, respectively), *E. coli* (24 independent clinical isolates for each antibiotic), or *A. baumannii* (24 clinical isolates for each antibiotic) treated at CLSI breakpoint concentrations with meropenem, ciprofloxacin, or gentamicin (the same isolates shown in Fig. 1b, c and Supplemental Fig. 1b, c). By definition, an SPD of 0 indicates a transcriptional response to antibiotic equivalent to that of an average susceptible strain, while an SPD of 1 indicates a response equivalent to that of an average resistant strain. See Supplementary Methods for details. Data are summarized as box-and-whisker plots, where boxes extend from the 25$^{th}$ to 75$^{th}$ percentile for each category, with a line at the median, and whiskers extend from the minimum to the maximum. Note that for *A. baumannii* and meropenem, the clustering of the majority of susceptible strains by this simple metric (aside from one outlier which is misclassified as resistant by GoPhAST-R) underscores the true differences in transcription between susceptible and resistant isolates, despite the more subtle-appearing differences in heatmaps for this combination (Supplemental Fig. 1b), which is largely caused by one strain with an exaggerated transcriptional response (seen here as the strain with a markedly negative SPD) that affects scaling of the heatmap. (b) The same SPD data (y-axes) plotted against broth microdilution MICs (x-axes) reveal that the magnitude of the transcriptional response to antibiotic exposure correlates with MIC. In both (a) and (b), strains with a large inoculum effect upon meropenem treatment are displayed in red and enlarged. Vertical dashed line indicates the CLSI breakpoint between susceptible and not susceptible (that is, intermediate or resistant).

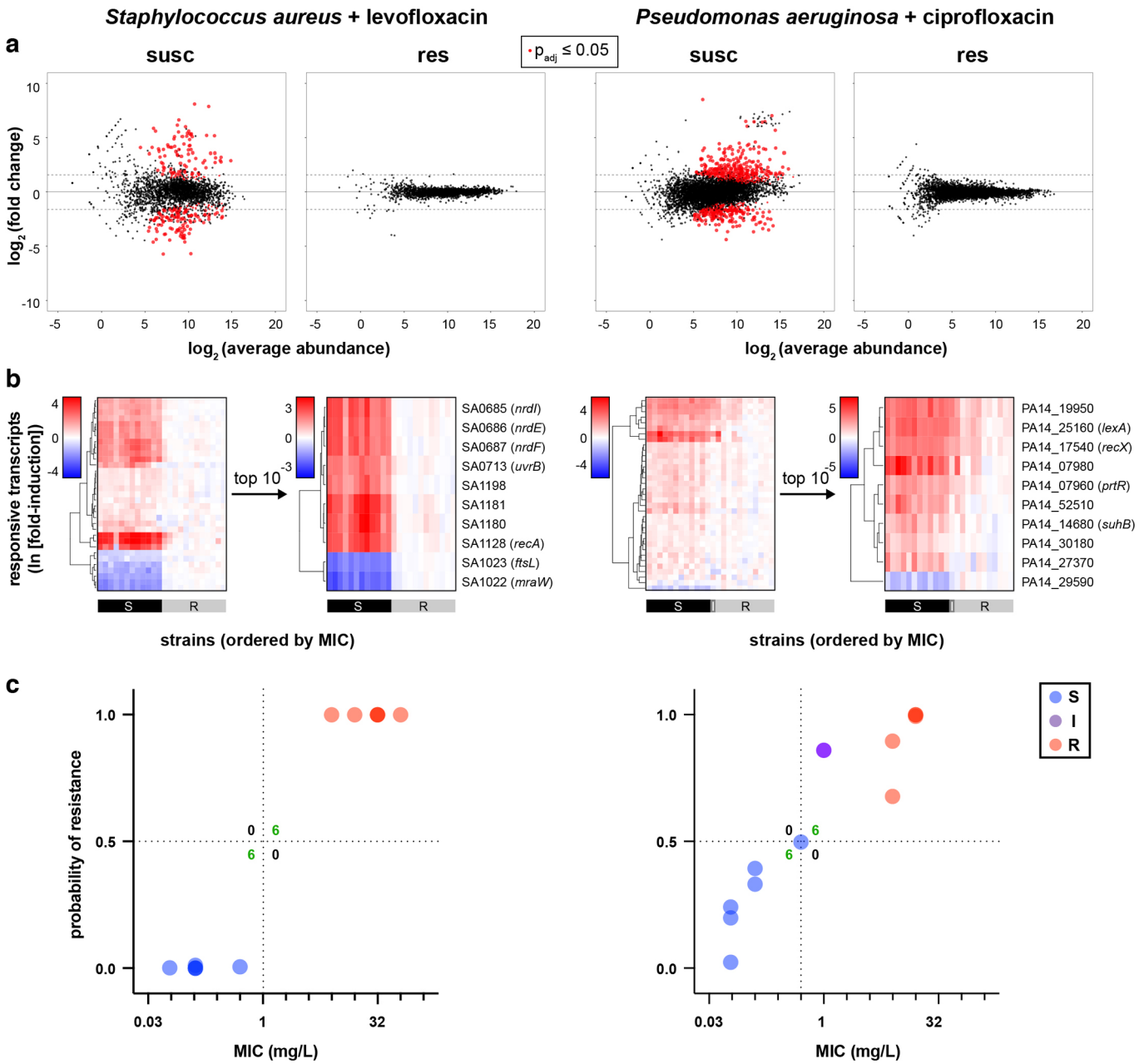


**Extended Data Fig. 6 | RNA-Seq and NanoString data reveal differential gene expression that distinguishes susceptible from resistant clinical isolates for *S. aureus* + levofloxacin and *P. aeruginosa* + ciprofloxacin.** (a) RNA-Seq data from two susceptible or two resistant clinical isolates of each species treated with the indicated fluoroquinolone at 1 mg/L for 60 minutes are presented as MA plots. Statistical significance was determined by a two-sided Wald test with the Benjamini-Hochberg correction for multiple hypothesis testing, using the DESeq2 package[28]. (b) Heatmaps of normalized, log-transformed fold-induction of antibiotic-responsive transcripts from 24 independent clinical isolates of each species treated with the indicated fluoroquinolone at 1 mg/L for 60 minutes. For each species, NanoString data from all candidate transcripts are shown at left, and top the 10 transcripts selected from Phase 1 testing are shown at right. (c) GoPhAST-R predictions of probability of resistance from a random forest model trained on Phase 1 NanoString data from the derivation cohort and tested on the validation cohort (y-axis) compared with standard CLSI classification based on broth microdilution MIC (x-axis). Horizontal dashed lines indicate 50% probability of resistance. Vertical dashed lines indicate the CLSI breakpoint between susceptible and not susceptible (that is intermediate/resistant). Numbers in each quadrant indicate concordant and discordant classifications between GoPhAST-R and broth microdilution.

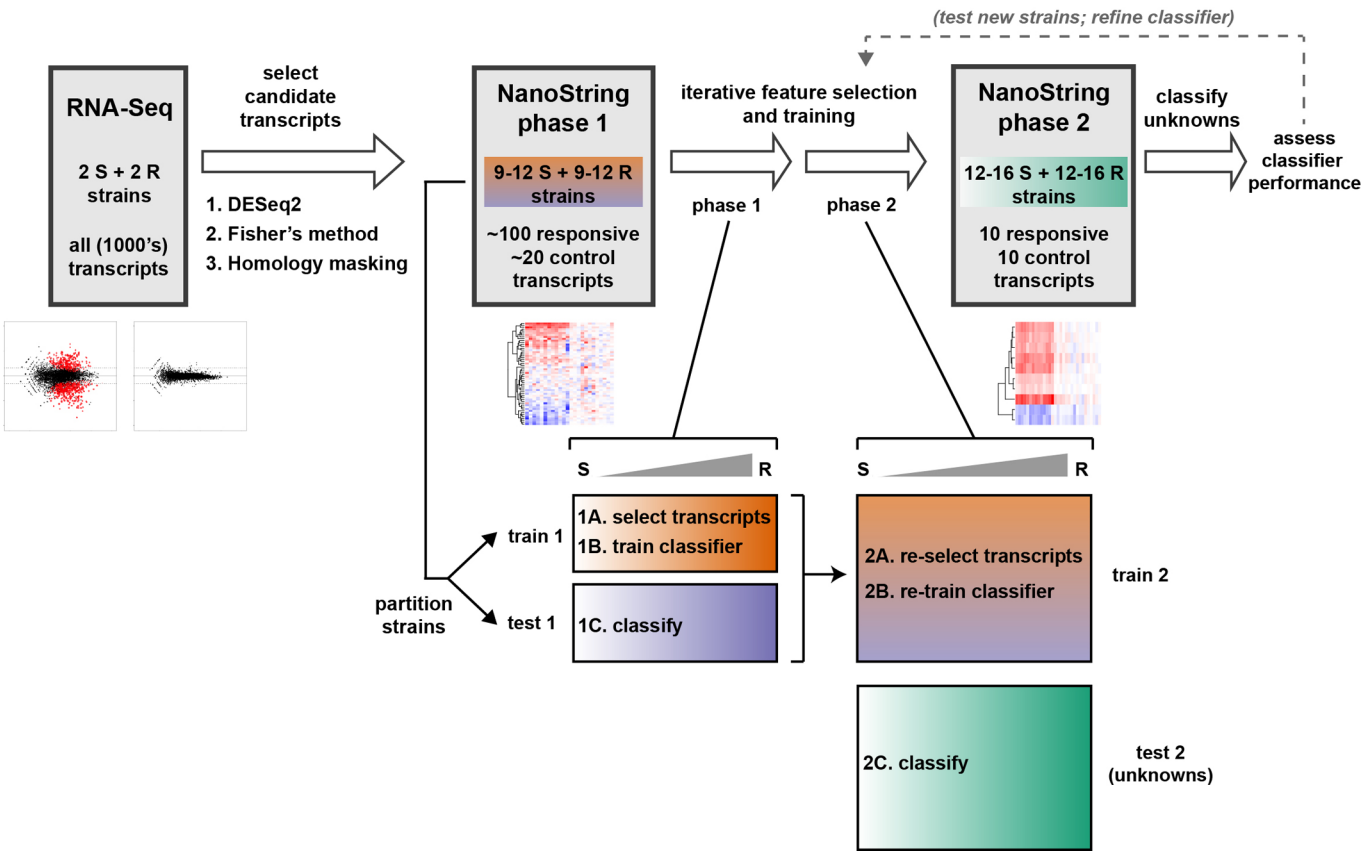


**Extended Data Fig. 7 | Schematic of data analysis scheme, including 'two-phase' machine learning approach to feature selection and strain classification.** Schematic representation of major data analysis steps in identifying antibiotic-responsive transcriptional signatures from RNA-Seq data, validating and optimizing these signatures using NanoString in two phases, and using these signatures to classify strains of unknown MIC, also in two phases. First, candidate antibiotic-responsive and control transcripts were chosen from RNA-Seq data using custom scripts built around the DESeq2 package[47], and conserved regions of these transcripts were identified for targeting in a hybridization assay. In phase 1 (implemented for all pathogen-antibiotic pairs), these candidate transcripts were quantitated on the NanoString assay platform, and the resulting data were partitioned by strain into training and testing cohorts. Ten transcripts that best distinguish susceptible from resistant strains within the training cohort were then selected (step 1A) using the reliefF feature selection algorithm (implemented via the CORElearn package), then used to train an ensemble classifier (step 1B) on the same training cohort using a random forest algorithm (implemented via the caret package). This trained classifier was then used to predict susceptibilities of strains in the testing cohort (step 1C), and accuracy was assessed by comparing with broth microdilution results (Supplementary Table 4). In phase 2 (implemented for *K. pneumoniae* + meropenem and ciprofloxacin), the same process was repeated, but the phase 1 training and testing cohorts were combined into a single, larger training cohort for feature selection (step 2A) and classifier training (step 2B), and a new set of strains were obtained as a testing cohort. The 10 genes selected from the phase 2 training cohort were measured from this phase 2 testing cohort, and the trained classifier was used for AST on these new strains (step 2C), with accuracy again assessed by comparison with broth microdilution (Supplementary Table 4). See Supplementary Methods for detailed descriptions of each of these analysis steps.

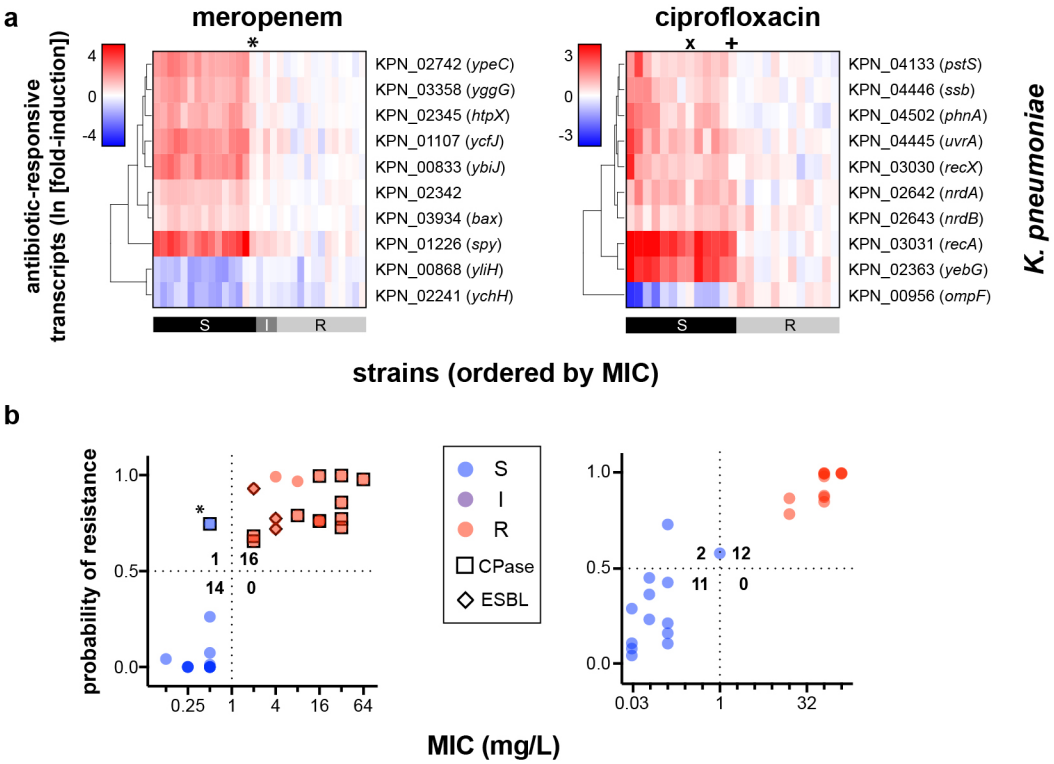


**Extended Data Fig. 8 | GoPhAST-R accurately classifies *K. pneumoniae* isolates tested in phase 2.** (a) Heatmaps of normalized, log-transformed fold-induction of top 10 antibiotic-responsive transcripts from *K. pneumoniae* treated at CLSI breakpoint concentrations with meropenem (31 independent clinical isolates) or ciprofloxacin (25 independent clinical isolates). CLSI classifications are shown below. * = strain with large inoculum effects in meropenem MIC; + = one-dilution error; x = strain discordant by more than one dilution. Note that the 10 responsive transcripts shown are the only 10 tested for this second phase of GoPhAST-R implementation. (b) GoPhAST-R predictions of probability of resistance from a random forest model trained on all Phase 1 NanoString data the independent Phase 2 cohort (y-axis) compared with standard CLSI classification based on broth microdilution MIC (x-axis). Horizontal dashed lines indicate 50% probability of resistance. Vertical dashed lines indicate the CLSI breakpoint between susceptible and not susceptible (that is intermediate/resistant). Numbers in each quadrant indicate concordant and discordant classifications between GoPhAST-R and broth microdilution. * = strain with large inoculum effects in meropenem MIC.

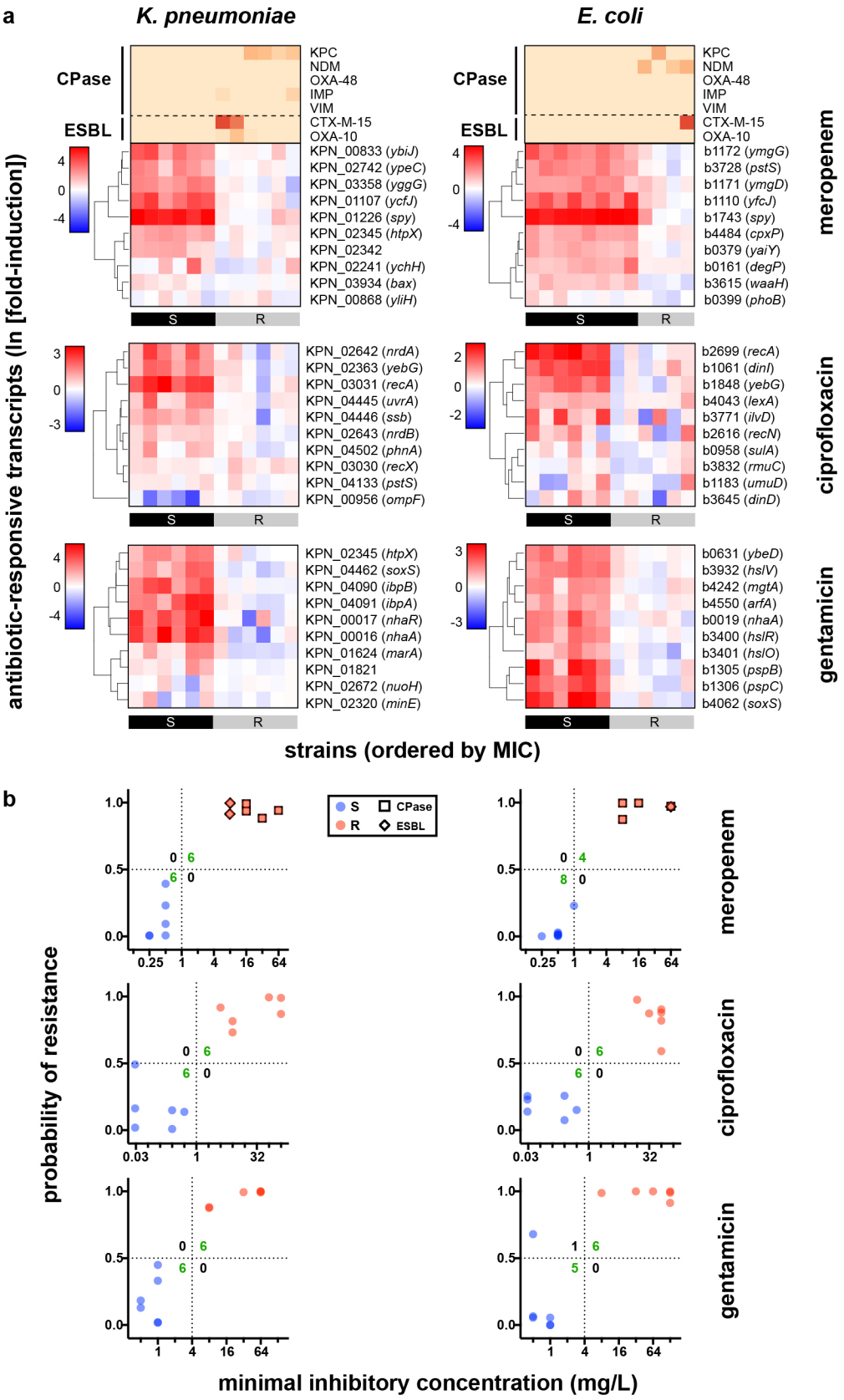


**Extended Data Fig. 9 |** See next page for caption.

**Extended Data Fig. 9 | GoPhAST-R accurately classifies AST and detects key resistance elements directly from simulated positive blood culture bottles in < 4 h.** (a) Heatmaps of normalized, log-transformed fold-induction NanoString data from the top 10 antibiotic-responsive transcripts directly from 12 simulated positive blood culture bottles for each indicated pathogen-antibiotic combination reveal antibiotic-responsive transcription in susceptible but not resistant isolates. For meropenem, results of carbapenemase / ESBL gene detection are also displayed as a normalized, background-subtracted, log-transformed heatmap above. CLSI classifications of isolates, which were blinded until analysis was complete, are displayed below each heatmap. (b) Probability of resistance from a random forest model trained by leave-one-out cross-validation on NanoString data from (a) (y-axis) compared with standard CLSI classification based on broth microdilution MIC (x-axis) for each isolate. Horizontal dashed lines indicate 50% chance of resistance based on random forest model. Vertical dashed lines indicate CLSI breakpoint between susceptible and resistant. Carbapenemase (square outline) and select ESBL (diamond outline) gene content as detected by GoPhAST-R are also displayed on meropenem plots. See Supplementary Methods for details of spike-in protocol.

nature research

Corresponding author(s): Deborah T. Hung

Last updated by author(s): Sep 26, 2019

# Reporting Summary

Nature Research wishes to improve the reproducibility of the work that we publish. This form provides structure for consistency and transparency in reporting. For further information on Nature Research policies, see Authors & Referees and the Editorial Policy Checklist.

## Statistics

For all statistical analyses, confirm that the following items are present in the figure legend, table legend, main text, or Methods section.

| n/a | Confirmed | |
|---|---|---|
| ☐ | ☒ | The exact sample size (*n*) for each experimental group/condition, given as a discrete number and unit of measurement |
| ☐ | ☒ | A statement on whether measurements were taken from distinct samples or whether the same sample was measured repeatedly |
| ☐ | ☒ | The statistical test(s) used AND whether they are one- or two-sided<br>*Only common tests should be described solely by name; describe more complex techniques in the Methods section.* |
| ☒ | ☐ | A description of all covariates tested |
| ☐ | ☒ | A description of any assumptions or corrections, such as tests of normality and adjustment for multiple comparisons |
| ☐ | ☒ | A full description of the statistical parameters including central tendency (e.g. means) or other basic estimates (e.g. regression coefficient) AND variation (e.g. standard deviation) or associated estimates of uncertainty (e.g. confidence intervals) |
| ☐ | ☒ | For null hypothesis testing, the test statistic (e.g. *F*, *t*, *r*) with confidence intervals, effect sizes, degrees of freedom and *P* value noted<br>*Give P values as exact values whenever suitable.* |
| ☒ | ☐ | For Bayesian analysis, information on the choice of priors and Markov chain Monte Carlo settings |
| ☐ | ☒ | For hierarchical and complex designs, identification of the appropriate level for tests and full reporting of outcomes |
| ☐ | ☒ | Estimates of effect sizes (e.g. Cohen's *d*, Pearson's *r*), indicating how they were calculated |

*Our web collection on statistics for biologists contains articles on many of the points above.*

## Software and code

Policy information about availability of computer code

| | |
|---|---|
| Data collection | NanoString data was collected using nSolver Analysis software (v4.070, NanoString, Seattle, Washington, USA). |
| Data analysis | RNA-Seq data were aligned using bwa (v0.7.17) and tabulated as previously described (Shishkin et al, Nat Meth 2015;12:323). Optimal transcripts were selected from RNA-Seq data using custom scripts described in this manuscript and deposited at https://github.com/broadinstitute/GeneSelection/ , built on the DESeq2 package (v1.10.1). GO terms were assigned and enrichment computed using blast2GO (v1.4.4). NanoString data were processed as described in this manuscript using R (v3.3.3), utilizing the packages dplyr (v0.7.4), xlsx (v0.5.7), gplots (v3.0.1), and DescTools (v0.99.23). Optimal NanoString probes/targets were identified, and strains were classified as susceptible or resistant, using custom scripts described in this manuscript and deposited at https://github.com/broadinstitute/DecisionAnalysis/ , implementing the COREIearn (v1.52.0) and caret (v6.0-78) packages in R (v3.3.3). |

For manuscripts utilizing custom algorithms or software that are central to the research but not yet described in published literature, software must be made available to editors/reviewers. We strongly encourage code deposition in a community repository (e.g. GitHub). See the Nature Research guidelines for submitting code & software for further information.

## Data

Policy information about availability of data

All manuscripts must include a data availability statement. This statement should provide the following information, where applicable:

- Accession codes, unique identifiers, or web links for publicly available datasets
- A list of figures that have associated raw data
- A description of any restrictions on data availability

All RNA-Seq data generated and analyzed during this study, supporting the analyses in Figure 1 and Figure S1, have been deposited as aligned bam files in the NCBI Sequencing Read Archive under study ID PRJNA518730. All other datasets generated during the current study, including raw and processed NanoString data, are available from the corresponding author on reasonable request.

# Field-specific reporting

Please select the one below that is the best fit for your research. If you are not sure, read the appropriate sections before making your selection.

☒ Life sciences ☐ Behavioural & social sciences ☐ Ecological, evolutionary & environmental sciences

For a reference copy of the document with all sections, see nature.com/documents/nr-reporting-summary-flat.pdf

# Life sciences study design

All studies must disclose on these points even when the disclosure is negative.

| | |
|---|---|
| Sample size | Sample sizes (i.e. number of strains tested) for RNA-Seq experiments were based on practical feasibility given the number of timepoints and treatment conditions desired, with clinical replicates in each case as described in the manuscript. Based on prior experience with antibiotic timecourses, and supported by data in this manuscript, two clinical replicates each of susceptible and resistant isolates for each bacteria-antibiotic pair was sufficient to identify hundreds of differentially expressed genes from these timecourses. Sample sizes (i.e., number of strains tested) for NanoString experiments were chosen to ensure a large enough sample size that five-fold cross-validation in the random forest model showed stable accuracy. The sample size for some bacteria-antibiotic pairs was constrained by availability of strains of the appropriate antibiotic resistance phenotype. Strains were also selected to represent a range of minimal inhibitory concentrations that span the clinical breakpoint concentration for each antibiotic, overweighted for strains near the breakpoint (i.e. not reflecting a natural distribution of isolates) in order to test performance on cases near the margin between susceptible and resistant. In both cases, rigorous statistical analysis was performed as described using published tools in order to support the conclusions in the manuscript: DESeq2 for differential expression of RNA-Seq data, and machine learning algorithms (reliefF and random forest) for feature selection and strain classification from NanoString data. |
| Data exclusions | No data were excluded from the analyses in this manuscript. |
| Replication | 23 of 24 Klebsiella pneumoniae strains tested for meropenem susceptibility in phase 1 NanoString experiments were retested in phase 2 using the smaller, targeted probeset. All 23 were correctly classified on retesting, with a Pearson correlation of 0.95 between the probability of resistance predicted by the random forest classifier for the same strains upon phase 1 vs phase 2 testing. See Supplemental Text (section entitled "Reproducibility of GoPhAST-R classification") for detail. |
| Randomization | As described in detail in the manuscript, randomization for training and testing cohorts in machine learning algorithms for feature selection and classification were done by arranging strains in order of minimal inhibitory concentration, then alternating assignments to training and testing. |
| Blinding | Cohort allocations of each strain were performed only after all data were collected, so all researchers were blinded during data collection. Susceptible or resistant designations for each strain in the testing (validation) cohort were blinded during classification algorithms and only revealed after classifier output was generated. Susceptibility classifications of clinical blood culture samples and spike-ins were blinded from all researchers and known only to clinical collaborators (J.S., V.M.P.) until all analysis was complete and classification predictions made; only then were the identities of the samples unblinded for comparison of conventional assays with GoPhAST-R results. |

# Reporting for specific materials, systems and methods

We require information from authors about some types of materials, experimental systems and methods used in many studies. Here, indicate whether each material, system or method listed is relevant to your study. If you are not sure if a list item applies to your research, read the appropriate section before selecting a response.

## Materials & experimental systems

| n/a | Involved in the study |
|---|---|
| ☒ | ☐ Antibodies |
| ☒ | ☐ Eukaryotic cell lines |
| ☒ | ☐ Palaeontology |
| ☒ | ☐ Animals and other organisms |
| ☐ | ☒ Human research participants |
| ☒ | ☐ Clinical data |

## Methods

| n/a | Involved in the study |
|---|---|
| ☒ | ☐ ChIP-seq |
| ☒ | ☐ Flow cytometry |
| ☒ | ☐ MRI-based neuroimaging |

## Human research participants

Policy information about studies involving human research participants

| | |
|---|---|
| Population characteristics | Bacterial isolates, and aliquots from clinical blood culture bottles, were collected from the clinical microbiology laboratories of Massachusetts General Hospital and Brigham and Women's Hospital without any knowledge of or selection for or against any characteristics of the patients from whom they were derived. The only parameters from the medical record that were collected were bacterial species identity and antibiotic susceptibility profiles; no identifying patient information was collected by |

| | |
|---|---|
| | researchers. |
| Recruitment | Patients were not recruited for any portion of this study; rather, clinical bacterial isolates or aliquots from clinical blood culture bottles were gathered directly from clinical microbiology laboratories as described above, under waiver of consent as approved by the Partners Health Care Institutional Review Board (IRB). |
| Ethics oversight | Partners Health Care IRB protocol 2015P002215 |

Note that full information on the approval of the study protocol must also be provided in the manuscript.